JOC The Journal of Organic Chemistry

Article

pubs.acs.org/joc

# $^{15}$N NMR Spectroscopy, X-ray and Neutron Diffraction, Quantum-Chemical Calculations, and UV/vis-Spectrophotometric Titrations as Complementary Techniques for the Analysis of Pyridine-Supported Bicyclic Guanidine Superbases

Ryan J. Schwamm,[†] Robert Vianello,*[,‡] Aleksandra Maršavelski,[‡] M. Ángeles García,[§] Rosa M. Claramunt,[§] Ibon Alkorta,[∥] Jaan Saame,[⊥] Ivo Leito,[⊥] Christopher M. Fitchett,[#] Alison J. Edwards,[⊗] and Martyn P. Coles*[,†]

[†]School of Chemical and Physical Sciences, Victoria University of Wellington, P.O. Box 600, Wellington 6012, New Zealand

[‡]Computational Organic Chemistry and Biochemistry Group, Ruder Bošković Institute, Bijenička cesta 54, 10000 Zagreb, Croatia

[§]Departamento de Química Orgánica y Bio-Orgánica, Facultad de Ciencias, UNED, Paseo Senda del Rey 9, 28040 Madrid, Spain

[∥]Instituto de Química Médica (IQM-CSIC), Juan de la Cierva 3, 28006 Madrid, Spain

[⊥]Institute of Chemistry, University of Tartu, 14a Ravila Street, 50411, Tartu, Estonia

[#]Department of Chemistry, University of Canterbury, Christchurch 8041, New Zealand

[⊗]Bragg Institute, Australian Nuclear Science and Technology Organization, Locked Bag 2001, Kirrawee DC, NSW 2234, Australia

Supporting Information

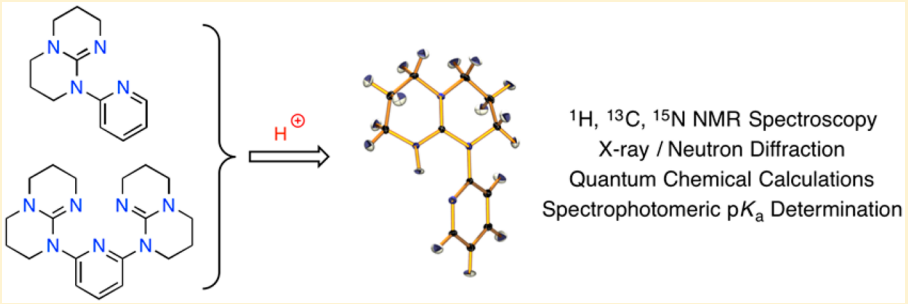


**ABSTRACT:** Pyridine substituted with one and two bicyclic guanidine groups has been studied as a potential source of superbases. 2-{hpp}$C_5H_4N$ (**I**) and 2,6-{hpp}$_2C_5H_3N$ (**II**) (hppH = 1,3,4,6,7,8-hexahydro-2*H*-pyrimido[1,2-*a*]pyrimidine) were protonated using $[HNEt_3][BPh_4]$ to afford [**I**-H][$BPh_4$] (**1a**), [**II**-H][$BPh_4$] (**2**), and [**II**-$H_2$][$BPh_4$]$_2$ (**3**). Solution-state $^{1}$H and $^{15}$N NMR spectroscopy shows a symmetrical cation in **2**, indicating a facile proton-exchange process in solution. Solid-state $^{15}$N NMR data differentiates between the two groups, indicating a mixed guanidine/guanidinium. X-ray diffraction data are consistent with protonation at the imine nitrogen, confirmed for **1a** by single-crystal neutron diffraction. The crystal structure of **1a** shows association of two $[\mathbf{I}\text{-H}]^+$ cations within a cage of $[BPh_4]^-$ anions. Computational analysis performed in the gas phase and in MeCN solution shows that the free energy barrier to transfer a proton between imino centers in $[\mathbf{II}\text{-H}]^+$ is 1 order of magnitude lower in MeCN than in the gas phase. The results provide evidence that linking hpp groups with the pyridyl group stabilizes the protonation center, thereby increasing the intrinsic basicity in the gas phase, while the bulk prevents efficient cation solvation, resulting in diminished p$K_a$(MeCN) values. Spectrophotometrically measured p$K_a$ values are in excellent agreement with calculated values and confirm that **I** and **II** are superbases in solution.

## INTRODUCTION

The guanidine functionality has been widely used in the design of superbases.[1] In accordance with IUPAC recommendations, a superbase is commonly defined as a compound with basicity higher than that of 1,8-bis(dimethylamino)naphthalene, DMAN (more commonly known as "proton-sponge" **a**, Figure 1), which corresponds to a gas-phase proton affinity of 245.8 kcal mol$^{-1}$ and a p$K_a$[2] > 18.6 in acetonitrile.[3,4] Different substitution patterns can strongly influence the basicity of the guanidine unit (e.g., 1,1,3,3-tetramethylguanidine, TMG (**b**), p$K_a$ = 23.3),[5,6] and it has been shown[7] that groups able to form (multiple) intramolecular hydrogen bonds (IHBs) further enhance the basic properties (e.g., 1,2,3-tris(3-(dimethylamino)propyl)guanidine, tris-DMPG (**c**), p$K_a$ = 27.2).[8−10] Combining multiple substituted guanidine groups

**Received:** June 1, 2016
**Published:** August 5, 2016





DOI: 10.1021/acs.joc.6b01330
J. Org. Chem. 2016, 81, 7612−7625

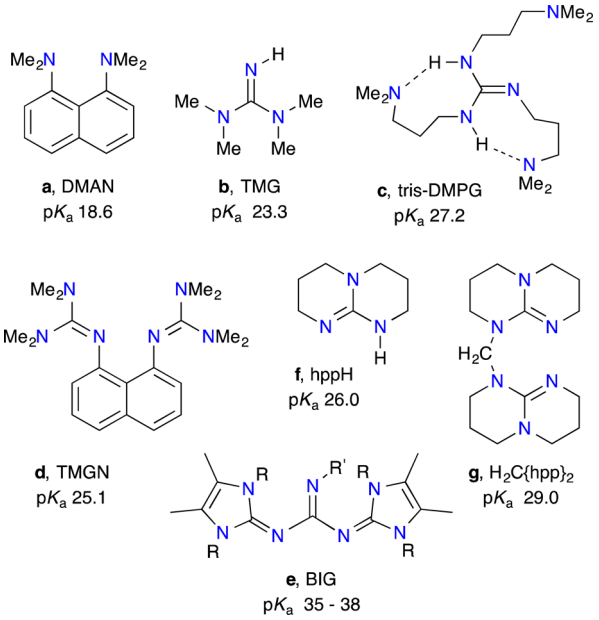


**Figure 1.** Selection of previously studied organic superbases relevant to this work.

about a common molecular scaffold can also increase the basicity (e.g., 1,8-bis(tetramethylguanidino)naphthalene, TMGN (**d**), p$K_a$ = 25.1),[6] provided there is a suitable pathway for charge transfer between the different units. For the conjugate acids of superbases, this involves proton transfer between functional groups. Similarly, extending the $\pi$-system of guanidine in a suitable way can lead to dramatic basicity increases, up to p$K_a$ 35−38 (e.g., *N*,*N*′-bis(imidazolyl)-guanidine, BIG (**e**)).[11]

1,3,4,6,7,8-Hexahydro-2*H*-pyrimido[1,2-*a*]pyrimidine, abbreviated as hppH or TBD,[12] is a bicyclic nitrogen-containing heterocycle in which the central guanidine component is incorporated into two fused six-membered rings (**f**). It has received attention as an organocatalyst in chemical transformations[13] and polymerization reactions[14] and has been used as a ligand in coordination chemistry.[15,16] In the context of this study, it is a known superbase with a p$K_a$ of 26.0.[3] The strong basic character derives from the conformationally rigid framework that locks the $\pi$-symmetry orbitals of the $CN_3$ core into a coplanar arrangement, facilitating charge delocalization.

We have shown that linking two hpp units with a methylene group to afford $H_2C\{hpp\}_2$ (**g**) produced a chelating ligand[17−19] and accessed unusual nucleophilic behavior of the hpp unit.[20,21] It also increased the basicity of the hpp groups by 3 orders of magnitude (p$K_a$ = 29.0)[22] due to a barrierless proton transfer between guanidinium/guanidine moieties.

Recently, Hanan and co-workers have synthesized a series of bi- and tridentate ligands combining pyridyl and hpp groups.[23] They were employed in the coordination chemistry of ruthenium and rhenium, focusing on the luminescent properties of the resultant compounds.[24−30] Inspired by a recent study of the incorporation of pyridyl substituents to form intramolecular hydrogen bonds to guanidinium units,[31] we initiated a study of how pendent pyridyl functionalities influence the basicity of the hpp unit. We report herein a combined experimental, structural (X-ray and neutron diffraction), and computational study of compounds **I** and **II** (Figure 2).

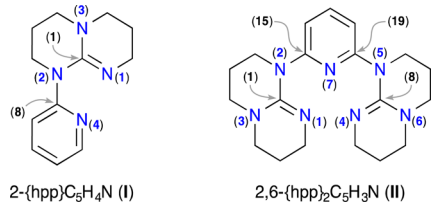


**Figure 2.** Pyridyl-substituted bicyclic guanidines showing the numbering scheme for nitrogen and selected carbon atoms.

## RESULTS AND DISCUSSION

**Synthesis.** The neutral compounds 2-$\{hpp\}C_5H_4N$ (**I**)[30] and 2,6-$\{hpp\}_2C_5H_3N$ (**II**)[25] were synthesized according to previously published procedures using palladium-catalyzed C−N bond-forming reactions.[32] Compound **I** was obtained as a colorless oil after workup (~90% pure by $^1$H NMR spectroscopy) and was used without further purification; compound **II** was obtained as colorless crystals. Monoprotonation of **I** and **II** was achieved with a stoichiometric amount of $[HNEt_3][BPh_4]$,[33] affording the tetraphenylborate salts, [2-$\{hppH\}C_5H_4N][BPh_4]$ ([**I**-H][$BPh_4$], **1a**) and [2-$\{hppH\}$-6-$\{hpp\}C_5H_3N][BPh_4]$ ([**II**-H][$BPh_4$], **2**), respectively (Schemes 1 and 2). The hexafluorophosphate salt [**I**-H][$PF_6$] (**1b**) was prepared as colorless crystals from the reaction of **I** with 1 equiv of $[NH_4][PF_6]$.

**Scheme 1. Synthesis of Monoprotonated Salts 1a and 1b**[a]

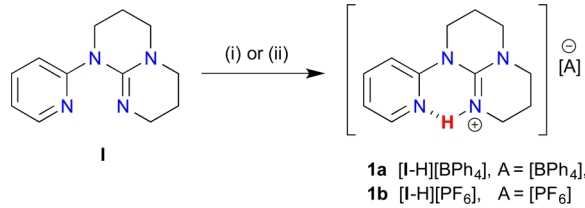


[a]Conditions: (i) $[HNEt_3][BPh_4]$, MeCN, 2 h; (ii) $[NH_4][PF_6]$, MeCN, 2 h.

**Scheme 2. Synthesis of Mono- and Diprotonated Salts 2 and 3**[a]

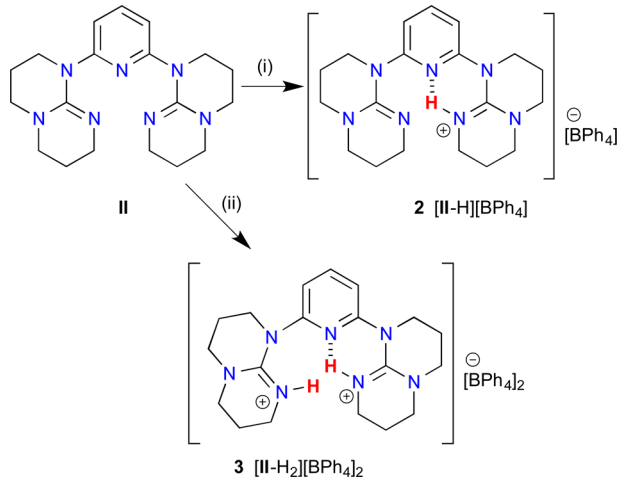


[a]Conditions: (i) $[HNEt_3][BPh_4]$ (1 equiv), MeCN, 1 h; (ii) $[HNEt_3][BPh_4]$ (2 equiv), MeCN, 1 h.



DOI: 10.1021/acs.joc.6b01330
J. Org. Chem. 2016, 81, 7612−7625

Although double protonation is not always straightforward in polyguanidyl systems,[6] we previously accessed the dication $[\mathbf{g}\text{-}H_2]^{2+}$ as the mixed chloride/tetraphenylborate salt from the reaction with $[HNEt_3][Cl]$, followed by anion-exchange with $Na[BPh_4]$.[18] The reaction of **II** with 2 equiv of $[HNEt_3][BPh_4]$ afforded the diprotonated salt $[2,6\text{-}\{hppH\}_2C_5H_3N][BPh_4]_2$ ($[\mathbf{II}\text{-}H_2][BPh_4]_2$, **3**) directly, without the need for an anion-exchange procedure (Scheme 2). Compounds **1**−**3** were obtained in yields exceeding 75%, and the elemental analyses were in agreement with the proposed formulas, demonstrating the bulk purity of the samples.

**Solution- and Solid-State NMR Studies.** *$^1$H NMR Analysis.* $^1$H NMR spectra of **1a** and **1b** in $CD_3CN$ show six resonances for the hpp-methylene groups, indicating nonsymmetrical substitution of the bicyclic framework. The N*H* resonance of the $[\mathbf{I}\text{-}H]^+$ cation ($\delta_H$ 9.47 and 9.43 for **1a** and **1b**, respectively) is deshielded compared with $[hppH(H)][BPh_4]$ ($\delta_H$ 5.76, no IHB in solid state) and is close to the corresponding hydrochloride salt [hppH(H)]Cl ($\delta_H$ 8.38, intermolecular NH···Cl in solid state).[34] The signals are, however, upfield of the methylene-bridged system $[H_2C\text{-}\{hppH\}\{hpp\}]^+$ ($[\mathbf{g}\text{-}H]^+$) in which the N*H* proton resonance at $\delta_H$ 13.51 was attributed to a strong IHB.[22]

Integration of the $^1$H NMR spectrum of the monoprotonated salt **2** ($CD_3CN$) indicates a single $[BPh_4]^-$ anion, in agreement with the proposed formula $[\mathbf{II}\text{-}H][BPh_4]$. The N*H* resonance was not observed in $CD_3CN$ but was present as a broad resonance at $\delta_H$ 9.70 in $CD_2Cl_2$. The NMR spectrum does not distinguish between the {hppH} and {hpp} groups, showing a single set of six overlapping resonances for both units. The *m*-$C_5H_3N$ environments are also equivalent, implying a symmetric $[\mathbf{II}\text{-}H]^+$ cation in solution. This is consistent with a number of possible (static) structures. Protonation of the pyridyl-nitrogen atom and retention of two neutral hpp units is considered unlikely given the relative basicities of these units ($pK_a$(hpp) = 26.03; $pK_a$(pyridine) = 12.5[35]). Formal protonation of one hpp group and generation of a symmetrical IHB, either with or without contribution from the pyridyl group, is also consistent with these data. However, given the low energies typically associated with proton transfer and solid-state X-ray and neutron diffraction data (vide infra), we propose that a dynamic process involving rapid exchange between tautomeric forms of $[\mathbf{II}\text{-}H]^+$ is present in solution (Scheme 3, (**i**)-a and (**i**)-b). Attempts to verify this by cooling a sample of **2** to −80 °C in $CD_2Cl_2$ were unsuccessful, with no significant change in line width observed in the $^1$H NMR spectrum (Figure S15). We conclude therefore that, if present, the proton shift is rapid on the NMR time scale.

**Scheme 3. Proposed Tautomeric Forms of $[\mathbf{II}\text{-}H]^+$**

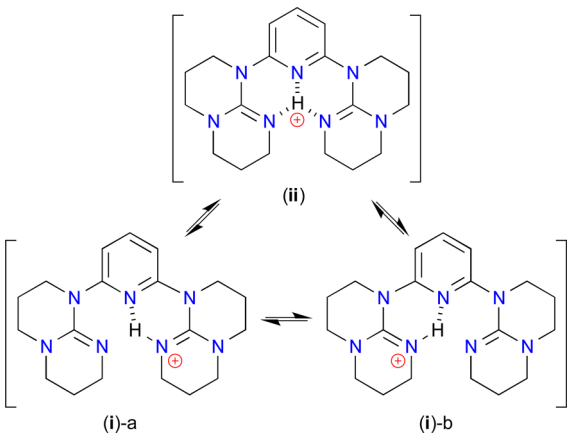


The $^1$H NMR spectrum of doubly protonated salt **3** also indicates a symmetrical cation, $[\mathbf{II}\text{-}H_2]^{2+}$, with equivalent "hppH" groups; integration for 2 equiv of $[BPh_4]^-$ is consistent with the postulated formula. The low solubility of the doubly charged salt in solution precluded observation of the N*H* proton in the $^1$H NMR spectrum.

*$^{15}$N NMR Analysis.* $^{15}$N NMR spectroscopy is a powerful analytical technique in the solid and solution states[36] and has been used previously to investigate pyridyl[37] and guanidyl systems.[38] We have reported the $^{15}$N NMR spectroscopic details for hppMe and the corresponding guanidinium cation $[hppMe(H)]^+$ in $CD_3CN$ (Table 1).[39] The key feature of the $^{15}$N NMR spectra of hppMe (entry 1) is the deshielded imine N atom ($\delta_{N1}$ −220.5) compared to the remaining nitrogens of the guanidine functionality. Protonation in situ to afford $[hppMe(H)]^+$ (entry 2), gave a large upfield shift for N1 ($\delta_{N1}$ −309.9; $\Delta\delta_{N1}$ = −89.4, entry 3), consistent with a change in the contribution from the sp$^2$-hybridized lone pair on protonation.[40]

**Table 1. $^{15}$N NMR Data ($CD_3CN$ Solution and CPMAS) for 2-{hpp}$C_5H_4N$ (I) and $[2\text{-}\{hppH\}C_5H_4N][BPh_4]$ (1a), Presented with Those for Neutral and Protonated hppMe (Refer to Figure 2 for Labeling Scheme)**

| | | N1 | N2 | N3 | N4 |
|---|---|---|---|---|---|
| 1[a] | hppMe | −220.5 | −318.9 | −311.5 | |
| 2[a,b] | $[hppMe(H)]^+$ | −309.9 | −305.4 | −299.8 | |
| 3 | $\Delta\delta_{(H+solution)}$ | −89.4 | +13.5 | +11.7 | |
| 4[a] | **I** | −207.3 | −278.4 | −308.1 | −96.2 |
| 5[a] | **1a** | −298.5 | −281.9 | −295.3 | −96.7 |
| 6 | $\Delta\delta_{(H+solution)}$ | −91.4 | +3.1 | +12.8 | −0.5 |
| 7[c] | **1a** | −297.2 | −277.9 | −286.6 | −96.7 |
| 8[d] | | *−293.6* | *−276.1* | *−290.0* | *−104.9* |

[a] $CD_3CN$. [b] +1 drop trifluoroacetic acid. [c] CPMAS. [d] Calculated values (*italics*).

The $^{15}$N NMR spectrum of **I** in $CD_3CN$,[41] shows a similar chemical shift pattern to hppMe (entry 4), with the highest frequency guanidine resonance corresponding to the imine nitrogen ($\delta_{N1}$ −207.3). The peak for the pyridyl nitrogen ($\delta_{N4}$ −96.2) indicates a more shielded environment when compared with the parent pyridine ($\delta_N$ −64).[42] The $^{15}$N NMR spectrum of **1a** in $CD_3CN$ (entry 5) shows the expected upfield shift for the N1 resonance ($\Delta\delta_{N1}$ = −91.4, entry 6), consistent with protonation at the imine nitrogen. A small but meaningful downfield shift of +12.8 ppm is also observed for the N3 resonance. Considering three possible resonance structures, *α*-, *β*-, and *γ*-, for the protonated guanidinium group (Scheme 4) and correlating these with a change in the hybridization of the nitrogen atom, this chemical shift difference is consistent with a large contribution from the *γ*-resonance form. No significant change is observed for the pyridyl nitrogen resonance, implying that this group plays a minimal role in delocalizing the charge of the $[\mathbf{I}\text{-}H]^+$ cation. The CPMAS results and the calculated values (entries 7 and 8) correspond well with those obtained in solution, suggesting similar structures are present in both states.

Both of the hpp groups in the neutral compound **II** are equivalent in solution by $^{15}$N NMR spectroscopy (Table 2,


DOI: 10.1021/acs.joc.6b01330
J. Org. Chem. 2016, 81, 7612−7625

**Scheme 4. Resonance Forms of the Protonated Guanidinium Component of [I-H]$^+$**

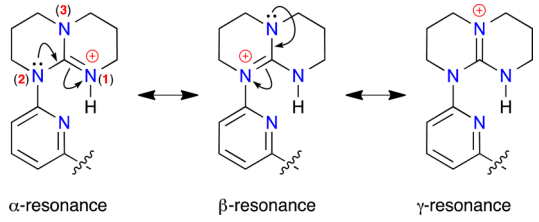


entry 1). The imine nitrogen atoms resonate at −206.1 ppm, similar to the corresponding resonance in **I**. The presence of two guanidine substituents gives a more shielded pyridyl resonance at −116.8 ppm. The $^{15}$N NMR spectrum of **2** in $CD_3CN$ (entry 2) shows equivalent guanidine moieties, as discussed above for $^1$H NMR spectroscopy. The N1/4 resonance appears at −280.7 ppm (entry 2) corresponding to a low frequency shift of −74.6 ppm (entry 3). This is considerably larger than predicted for the average signal of a protonated (N1) and nonprotonated (N4) imine nitrogen atom based on the results in Table 1, where average values of −44.7 ppm and −45.7 ppm for the hppMe and **I** systems are calculated for $\{\Delta\delta_{(H+solution)}/2\}$. This indicates that both of the imine nitrogens are affected by the presence of the proton in [**II**-H]$^+$, consistent with a dynamic exchange between tautomeric forms (Scheme 3). The low field shift of +7.2 ppm for the pyridyl resonance, larger than observed in **I**/**1a**, suggests that this atom may also play a role in the delocalization process (i.e., **ii**, Scheme 3).

In solution, the average signal for the protonated imine nitrogens of **3** resonate at −300.1 ppm (entry 4), consistent with the $\Delta\delta_N$ values extrapolated from values for hppMe and **I**. The pyridyl nitrogen peak is shifted downfield by +9.9 ppm (entry 5), which may also suggest a contribution from this group to the solution-state structure. The N3/6 chemical shifts for monoprotonated **2** and diprotonated **3** are both deshielded (+11.0 ppm and +15.0 ppm, respectively), also consistent with the γ-resonance playing a key role in the guanidinium structure.

The CPMAS $^{15}$N NMR spectra of **II** distinguish between the two crystallographically different hpp groups (entry 6, Figure 3).[24] Monoprotonation to afford **2** (entry 8) gives the expected upfield shift for one of the imine nitrogen resonances (entry 10) with a chemical shift difference $\Delta\delta_{N1}$ of −106.4 ppm. The formally nonprotonated imine nitrogen N4 also experiences a shielding effect of −10.1 ppm (Figure 3). The pyridyl resonance shifts to higher frequency by +15.2 ppm, almost

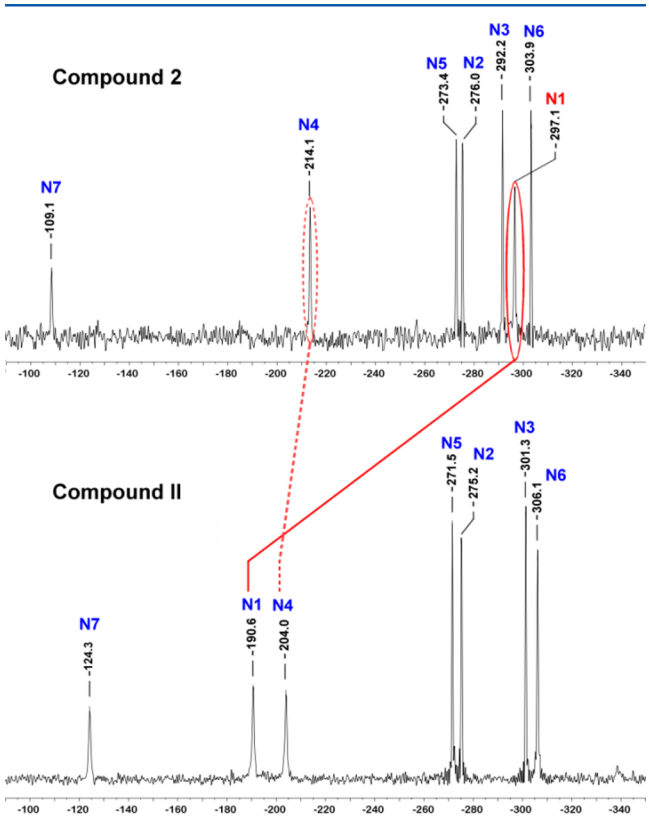


**Figure 3.** $^{15}$N CPMAS spectra of 2,6-{hpp}$_2$C$_6$H$_3$N (**II**, bottom) and [2-{hppH}-6-{hpp}C$_6$H$_3$N][BPh$_4$] (**2**), highlighting the upfield shift of the two imino-nitrogen atoms.

**Table 2. $^{15}$N NMR Data ($CD_3CN$ Solution and CPMAS) for 2,6-{hpp}$_2$C$_5$H$_3$N (II), [2-{hppH}-6-{hpp}C$_5$H$_3$N][BPh$_4$] (2), and [2,6-{hppH}$_2$C$_6$H$_3$N][BPh$_4$]$_2$ (3) (Refer to Figure 2 for Labeling Scheme)**

| | | N1 | N2 | N3 | N4 | N5 | N6 | N7 |
|---|---|---|---|---|---|---|---|---|
| 1[a] | **II** | −206.1 | −279.8 | −308.4 | [e] | [e] | [e] | −116.8 |
| 2[a] | **2** | −280.7 | −282.0 | −297.4 | [f] | [f] | [f] | −109.6 |
| 3 | $\Delta\delta_{(H+solution)}$[d] | −74.6 | −2.2 | +11.0 | [e,f] | [e,f] | [e,f] | +7.2 |
| 4[a] | **3** | −300.1 | −282.5 | −293.4 | [f] | [f] | [f] | −106.9 |
| 5 | $\Delta\delta_{(H+solution)}$[d] | −94.0 | −2.7 | +15.0 | [e,f] | [e,f] | [e,f] | +9.9 |
| 6[b] | **II** | −190.6, | −275.2, | −301.3, | −204.0, | −271.5, | −306.1, | −124.3, |
| 7[c] | | *−185.4* | *−271.8* | *−301.8* | *−203.9* | *−270.9* | *−307.6* | *−136.2* |
| 8[b] | **2** | −297.1, | −276.0, | −292.2, | −214.1, | −273.4, | −303.9, | −109.1, |
| 9[c] | | *−291.4* | *−273.2* | *−297.5* | *−225.7* | *−272.8* | *−306.8* | *−106.8* |
| 10 | $\Delta\delta_{(H+solid)}$[d] | −106.4 | −0.7 | +9.1 | −10.1 | −1.9 | +2.3 | +15.2 |
| 11[b] | 3 | −288.7 | −275.2 | −281.3, | −288.7 | −276.2 | −279.4, | [g] |
| | | | | −278.2 | | | −281.3 | |
| 12[c] | | *−300.4,* | *−272.6,* | *−285.2,* | *−300.4,* | *−272.6,* | *−285.1,* | *−126.9,* |
| | | *−303.5* | *−272.8* | *−284.0* | *−300.4* | *−272.7* | *−285.1* | *−125.3* |
| 13 | $\Delta\delta_{(H+solid)}$[d] | −98.0 | 0.0 | +20.0 | −84.7 | −4.7 | +26.7 | – |

[a]$CD_3CN$. [b]CPMAS. [c]Calculated values (*italics*). [d]chemical shift difference ($\Delta\delta$) calculated relative to the neutral form. [e]N1/N4, N2/N5, and N3/N6 are equivalent in solution. [f]N1/N4, N2/N5, and N3/N6 are average values for the protonated and neutral guanidine groups. [g]Not observed.



DOI: 10.1021/acs.joc.6b01330
J. Org. Chem. 2016, 81, 7612−7625

Table 3. Selected Bond Lengths (Å) and Related Geometrical Parameters from Single-Crystal X-ray Data

| | 1a | 1b | II[a] | 2 | 3a[b] | 3b[b] | 3c[b] |
|---|---|---|---|---|---|---|---|
| C1−N1 (*x*)[c] | 1.331(2) | 1.325(2) | 1.278(3) | 1.334(1) | 1.331(3) | 1.324(3)[a] | 1.329(3)[a] |
| C1−N2 (*y*)[c] | 1.369(2) | 1.368(2) | 1.409(3) | 1.365(1) | 1.382(3) | 1.378(3)[a] | 1.384(3)[a] |
| C1−N3 (*z*)[c] | 1.330(2) | 1.327(2) | 1.383(3) | 1.336(1) | 1.328(3) | 1.337(3)[a] | 1.331(3)[a] |
| $N_{imine}\cdots N_{pyridyl}$ | 2.671(2) | 2.670(2) | 4.175(3) | 2.692(1) | 2.611(3) | 2.608(3) | 2.597(3) |
| C8−N4 (*x*)[c] | | | 1.260(3) | 1.287(1)[a] | 1.321(3)[a] | 1.329(3)[a] | 1.323(3)[a] |
| C8−N5 (*y*)[c] | | | 1.409(3) | 1.403(1)[a] | 1.382(3)[a] | 1.382(3)[a] | 1.382(3)[a] |
| C8−N6 (*z*)[c] | | | 1.388(3) | 1.377(1)[a] | 1.329(3)[a] | 1.330(3)[a] | 1.329(3)[a] |
| $N_{imine}\cdots N_{pyridyl}$ | | | 3.878(4) | 2.692(1) | 2.611(3) | 2.608(3) | 2.597(3) |
| | | | | 2.811(1) | 2.820(3) | 2.775(3) | 2.742(3) |
| $N_{imine}\cdots N_{imine}$ | | | | 3.129(1) | 3.768(3) | 3.634(3) | 3.450(3) |
| | | | Protonated Group(s) | | | | |
| Φ(1) | −42.56(16) | −38.0(2) | | −43.17(18) | 29.6(3) | −29.1(3) | 25.5(3) |
| | | | | | 20.8(3) | −19.5(3) | 19.7(3) |
| $\Delta_{CN}$ | 0.04 | 0.04 | | 0.03 | 0.05, 0.06 | 0.05, 0.05 | 0.06, 0.06 |
| $\Delta'_{CN}$ | −0.02 | −0.02 | | −0.01 | −0.03, − 0.02 | −0.01, − 0.03 | −0.03, − 0.02 |
| ρ | 0.99 | 0.98 | | 0.99 | 0.98, 0.97 | 0.98, 0.98 | 0.98, 0.98 |
| | | | Nonprotonated Group(s) | | | | |
| Φ(2) | | | −176.4(2) | 38.86(17) | | | |
| | | | 138.3(2) | | | | |
| $\Delta_{CN}$ | | | 0.13, 0.15 | 0.12 | | | |
| $\Delta'_{CN}$ | | | 0.04, 0.05 | 0.03 | | | |
| ρ | | | 0.91, 0.90 | 0.93 | | | |

[a]Different atom labeling scheme, corresponding bond lengths quoted. [b]Three independent molecules in the unit cell. [c]Labels (*x*), (*y*), and (*z*) refer to the bond lengths used to define $\Delta_{CN}$, $\Delta'_{CN}$ and ρ (see Figure 8).

double that noted in solution. The solid-state NMR spectrum of **3** (entry 11) is complicated by the presence of three molecules in the unit cell, each of which contains a disordered annular methylene group. The resonance for the pyridyl nitrogen atom could not be observed but is calculated at $\delta_{N7(calc'd)}$ − 126.9/−125.3 (entry 12). The expected upfield shift for the imine nitrogen atoms is observed (entry 13) with a magnitude consistent with the changes in the solution-state chemical shifts. As noted for the monosubstituted system, a relatively large chemical shift difference for the N3/6 resonances (**2**, $\Delta\delta_{N3}$ = +9.1; **3**, $\Delta\delta_{N3}$ = +20.0 and $\Delta\delta_{N6}$ = +26.7) is consistent with contribution from the γ-resonance to the overall bonding.

**Solid-State Structural Analysis.** *Single-Crystal X-ray Analysis.* Single-crystal X-ray diffraction experiments have been performed on **1a**, **1b**, **2**, and **3**; these data are compared with the crystal structure of **II**.[24] The cationic components [**I**-H]$^+$, [**II**-H]$^+$, and [**II**-H$_2$]$^{2+}$ (one of three in the unit cell) are shown in Figures 4−6, respectively; selected bond lengths and angles are collected in Table 3. In all cases, residual electron density consistent with the presence of a hydrogen atom at the protonated imine nitrogen was located on the difference map and freely refined.

Data for compound **1a** indicates the formula of the monoprotonated compound is the guanidinium salt, [2-{hppH}C$_5$H$_4$N][BPh$_4$] (Figure 4). The pyridyl ring is rotated relative to the planar CN$_3$ core of the guanidine, with a N4−C8−N2−C1 torsion angle Φ(1) of −42.56(16)°. The N1···N4 separation (2.671(2) Å) is shorter than in [H$_2$C{hppH}-{hpp}]$^+$ ([**g**-H]$^+$, 2.73 Å), indicating the presence of an IHB, although the nominal angle at the hydrogen atom is less than ideal (**1a**, 137(2)°; [**g**-H]$^+$, 168(3)°). Similar values were observed for the hexafluorophosphate salt **1b** (Φ(1) = −38.0(2)°; N1···N4 = 2.670(2) Å), although disorder within the annular methylene groups and [PF$_6$]$^-$ anion resulted in a less precise structural solution.

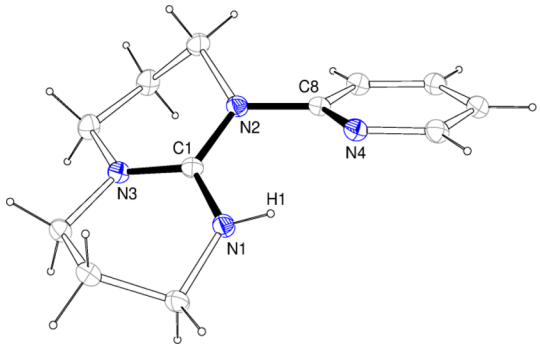


**Figure 4.** Displacement ellipsoid plot (30% probability) of the cationic component of [**I**-H][BPh$_4$] (**1a**).

Compound **2** consists of the ion pair [**II**-H][BPh$_4$] (Figure 5). Respectful of the limits of X-ray diffraction data, the N*H*

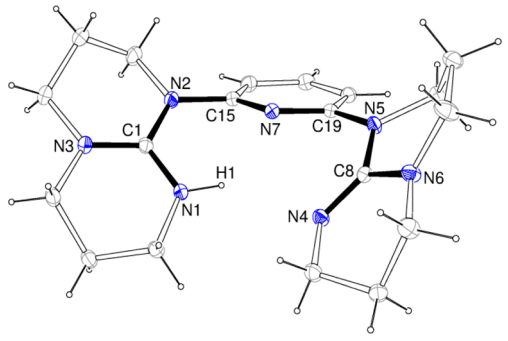


**Figure 5.** Displacement ellipsoid plot (30% probability) of the cationic component of [**II**-H][BPh$_4$] (**2**).



DOI: 10.1021/acs.joc.6b01330
J. Org. Chem. 2016, 81, 7612−7625

proton is assigned to one of the imine nitrogen atoms, generating a nonsymmetrical cation containing one protonated and one neutral hpp group. This conclusion is supported by differences in C−N bond lengths for the two hpp groups (vide infra). There is also a notable difference in the rotation of the guanidine moieties relative to the pyridyl ring, generating substantially different $N_{imine}\cdots N_{pyridyl}$ distances. The hppH fragment is orientated with torsion $\Phi(1) = -43.17(18)°$ and an N1···N7 distance of 2.692(1) Å (angle at hydrogen 132°), whereas the neutral hpp group has a corresponding torsion $\Phi(2) = 38.86(17)°$ and a greater N4···N7 distance of 2.811(1) Å. Both of the guanidine-based groups are rotated in the same direction relative to the $C_5H_5N$ ring with a resultant N1···N4 distance of 3.129(1) Å and a N−H···N angle of 148°. This conformation is the most favorable for any intramolecular proton transfer pathway.

Compound **3** crystallized with three $[\mathbf{II}\text{-}H_2]^{2+}$ ions in the unit cell (**3a**−**c**)[43] and six $[BPh_4]^-$ ions; minor disorder is present in one of the annular methylene groups of each of **3b** and **3c**. Within each dication, the hppH fragments are rotated such that the N*H* groups are on opposite sides of the plane defined by the pyridyl ring (Figure 6). The torsion angles of the

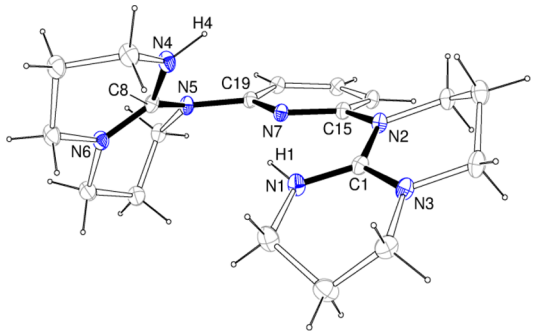


**Figure 6.** Displacement ellipsoid plot (20% probability) of dication **3a** from the structure of $[\mathbf{II}\text{-}H_2][BPh_4]_2$ (**3**).

two groups differ (avg $|\Phi(1)| = 28.1°$; avg $|\Phi(2)| = 20.0°$), with corresponding differences in the $N-H\cdots N_{pyridyl}$ distances (avg 2.61 and 2.78 Å, respectively). This distinction generates a planar-chiral structure in the solid state, with the two forms labeled ss-$S_p$ and ss-$R_p$ (Figure 7), based on the work of

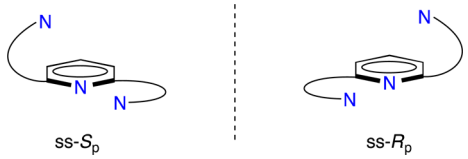


**Figure 7.** Schematic representation of the two solid-state planar-chiral isomers found in the dicationic $[\mathbf{II}\text{-}H_2]^{2+}$ component of the crystal structure of **3**.

Prelog,[44] and consistent with our previous work with ferrocene amidinium salts.[45] Cations **3a** and **3c** correspond to a ss-$S_p$ conformation (ss is defined as a solid-state phenomenon), and the guanidinum groups in **3b** are arranged with the ss-$R_p$ conformation. This difference does not result in significant differences in the bond lengths within the dicationic units and is therefore likely due to subtle crystal packing forces.

The previously defined parameters $\Delta_{CN}$,[46] $\Delta'_{CN}$,[47] and the $\rho$-ratio[48,49] offer a measure of the extent of delocalization within the $\pi$-system of hpp-based cations (Figure 8, Table 3).[22,34] The $\Delta_{CN}$ values for **II** (0.13 and 0.15 Å) are indicative of localization

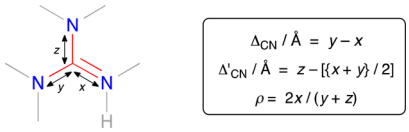


**Figure 8.** Definition of $\Delta_{CN}$, $\Delta'_{CN}$, and the $\rho$-ratio used to describe the bonding within the $CN_3$ core of the hpp unit.

of the amidine unit into C−N1 double and C−N2 single bonds. In all instances, protonation reduces this value (range 0.03 Å to 0.06 Å), consistent with an increase in delocalization of $\pi$-density across this fragment. There is also a notable decrease in the $\Delta'_{CN}$ values for the protonated species, consistent with contribution from the $\gamma$-resonance (Scheme 4); this agrees with $^{15}N$ NMR data (vide supra).

The $\rho$-ratios in **II** show that the C═N double bond length ($x$) is ∼90% of the average of the C−$NR_2$ single bonds ($y$ and $z$), typical for neutral hpp groups.[34] Protonation increases the value of $x$ with a concomitant decrease in $y$ and $z$ as the $\alpha$-, $\beta$-, and $\gamma$-resonance forms contribute to the bonding scheme until a $\rho$ ratio of 1.00 is calculated for a fully delocalized system ($x = y = z$). In this study, the $\rho$-ratios of the protonated hppH groups within **1a**/**b**, **2**, and **3** approach unity (range 0.97−0.99), consistent with previously studied systems.

Compared with the results calculated for **II**, the $\Delta_{CN}$, $\Delta'_{CN}$, and $\rho$-ratios of the formally neutral hpp group in **2** all show a small shift toward the values expected for a protonated system. Although we are unable to demonstrate that these structural data arise from "partial protonation" of the neutral guanidine,[49] in concert with the spectroscopic data we can confidently say that the bonding within this group is influenced by the protonation of the other guanidine. Similar observations were made with $[\mathbf{g}\text{-}H]^+$.[22]

*Single-Crystal Neutron Diffraction Study of Compound **1a**.* The X-ray diffraction data for the compounds described in this study are of high quality, allowing the positions of the carbon and nitrogen framework to be accurately determined. However, the low scattering power of hydrogen does not allow for the determination of its nuclear position with any confidence using this technique. This limitation is compounded in the study of hydrogen bonds as the electron density within the polarized D−H···A bonds is distorted, which can lead to inaccuracies of up to 0.15 Å for the D−H distance.[50] To overcome these limitations, crystals of **1a** were analyzed by single-crystal Laue neutron diffraction,[51,52] with data collected at the OPAL reactor using the KOALA instrument at the Bragg Institute, Australian Nuclear Science and Technology Organization (ANSTO). The results from this experiment allow the precise nuclear positions to be determined,[53,54] enabling the geometry of the IHB for a hpp-based system to be accurately assessed for the first time.

All hydrogen and non-hydrogen atoms were included in the refinement, giving satisfactory displacement ellipsoids (Figure 9). From this model, we can confirm that the hydrogen atom is exclusively located on the imino nitrogen atom N1, as inferred from X-ray diffraction data (vide supra). The N1−H11 bond length of 1.048(4) Å is ∼22% greater than that obtained from X-ray diffraction data (Table 4) and is long compared to the data presented for charged $N^+$-H groups in Allen and Bruno's 2010 review of CSD data (1.036 Å).[50] The corresponding


DOI: 10.1021/acs.joc.6b01330
J. Org. Chem. 2016, 81, 7612−7625

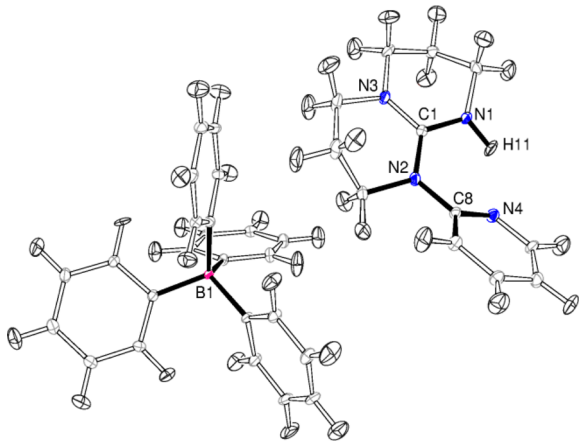


**Figure 9.** Displacement ellipsoid plot (30% probability) of **1a** generated from neutron diffraction data.

**Table 4. Selected Bond Lengths (Å) and Angles (deg) from [I-H]$^+$, Comparing Values Generated from Different Techniques**

| | X-ray | calcd (gas) | calcd (MeCN) | Neutron |
|---|---|---|---|---|
| N1−H | 0.86(2) | 1.027 | 1.018 | 1.048(4) |
| H···N4 | 1.98(2) | 1.774 | 1.865 | 1.846(5) |
| N1···N4 | 2.671(2) | 2.622 | 2.676 | 2.678(2) |
| N1−H···N4 | 137(2) | 137.2 | 134.2 | 133.6(5) |
| \|Φ(1)\| | 42.56(16) | 29.4 | 35.4 | 42.5(3) |
| H···H[a] | 2.1765(1) | 2.204 | 2.215 | 2.096(8) |

[a]Intramolecular H···H distance between the protons labeled H21 and H91 (see Figure 11).

reduction in the H···$N_{pyridine}$ IHB distance is ∼7% (1.846(5) Å), with the N1−H11···N4 angle 133.6(5)°. As expected, the differences in atomic positions are not as pronounced for the heavier atoms, with the N1···N4 distances indistinguishable (within 3$\sigma$) using the two techniques.

The accepted literature value for the van der Waals radius of hydrogen is 1.2 Å.[55] The high quality neutron diffraction data for **1a** allows us to examine the structure for the presence of H···H interactions that may influence the geometry, but are not normally assessed for X-ray derived models. To consider the full impact of such contacts it is important to first analyze the arrangement of cations and anions within the crystal structure.

The packing within the crystal structure of **1a** reveals a close association of two [**I**-H]$^+$ cations (about a crystallographic inversion center), surrounded by a cage of eight $[BPh_4]^-$ anions (Figure 10). This is unusual considering the positive charge in both species but has been examined computationally for guanidinium pairing in water[56] and recently reported in triaminocyclopropenium cations that form "$\pi$-dimers" in the solid state.[57] The interplane distance defined by the $CN_3$ core of the protonated units in the $([\mathbf{I}\text{-H}]_2)^{2+}$ cation pair is 3.512(3) Å, compared with $C_3$···$C_3$ centroid separations of 3.225(1) and 3.351(2) Å in the cyclopropenium system. The shortest intermolecular H···H distance (2.370(7) Å) is between protonated imine hydrogen (H11) and H22 from the C2 methylene of the adjacent cation (Figure 11). There is also a short H···H contact between the N*H* atom and an aryl proton of a borate anion, with the H11···H361 distance 2.240(9) Å.

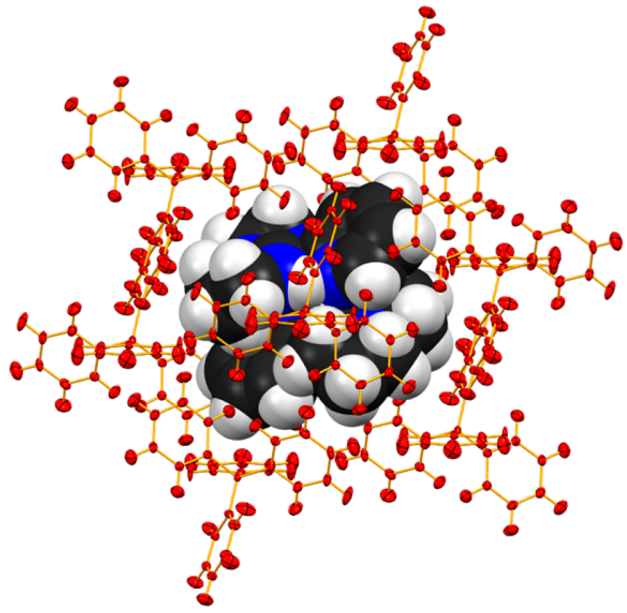

**Figure 10.** Section of the crystal structure of **1a** (neutron diffraction derived model) showing two cations (displayed as space-fill models) surrounded by a cage of eight anions (atoms displayed as red, 30% ellipsoids).

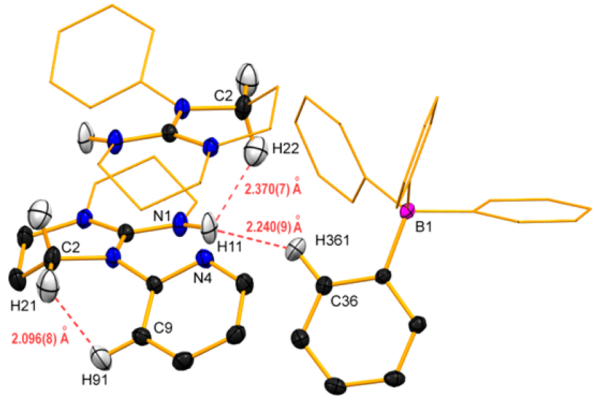


**Figure 11.** Inter- and intramolecular H···H contacts for [**I**-H]$^+$ (values from neutron diffraction derived model).

Examination of the *intra*molecular H···H contacts revealed from neutron diffraction data helped to explain a key structural feature of cation [**I**-H]$^+$, namely the origins of the torsion angle Φ(1). As expected, this value, −42.5(3)°, does not change between X-ray and neutron diffraction derived models. However, the proton positions clearly indicate a strong H···H interaction between H21 and H91 (2.096(8) Å, neutron data). This conflict is minimized by twisting the pyridyl group relative to the $CN_3$ core of the guanidinium component.

**Computational Analysis.** *General Considerations.* To examine the relative stabilities of the possible conformers of **1**, **2**, and **3** and their protonated forms, the parameters associated with the intramolecular hydrogen bond and the experimentally determined basicity, computational analysis has been performed. All results were obtained by the M06-2X/6-311++G(2df,2pd)//M06-2X/6-31+G(d,p) model,[58] with calculations both in the gas-phase and implicit acetonitrile solution. The M06-2X functional was developed to provide highly accurate thermodynamic and kinetic parameters for organic system,[59] and previously been shown to be very accurate in


DOI: 10.1021/acs.joc.6b01330
J. Org. Chem. 2016, 81, 7612−7625

estimating both p$K_a$ and reaction thermodynamic values in solution.[60,61] The calculations for hppMe and $H_2C\{hpp\}_2$ (**g**) have been repeated at this level of theory (previously performed using the B3LYP/6-311+G(2df,p)//B3LYP/6-31G(d) model)[22] to allow direct comparison with the results from this study. Further details and molecular coordinates are included in the Supporting Information.

*Monosubstituted Compounds Based on Compound I (Gas Phase).* In the neutral form, repulsion between the imino and pyridyl lone pairs of electrons is such that the most stable conformation of **I** is **1A** (Figure 12 and Table 5). Indeed, structure **1B** is not stable and during optimization proceeds with rotation about the C8−N2 bond (see Figure 2 for atom assignment) to afford **1A**. In agreement with experimental data, the calculated position for the first protonation is the imine nitrogen of the hpp group, which from the ground-state neutral structure **1A** affords **1B-H$^+$**. In the gas phase, this structure is unstable and isomerizes to **1A-H$^+$** to allow formation of an IHB. The resultant N1···N4 distance (2.622 Å) and N1−H···N4 angle (137.2°) are in excellent agreement with the experimentally observed values from X-ray and neutron diffraction derived models. Although the calculated torsion |Φ(1)| of 29.4° is considerably less than observed in the solid state, it confirms that the deviation from coplanarity has an energetic component and is not an artifact of crystal packing.

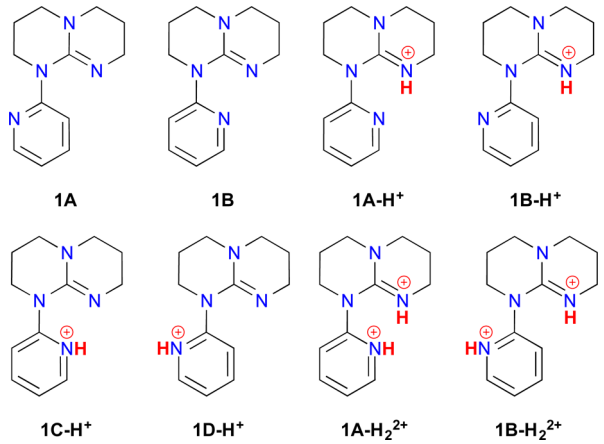


**Figure 12.** Conformers of **I**, [**I**-H]$^+$, and [**I**-$H_2$]$^{2+}$ used for computational analysis.

**Table 5. Calculated Gas-Phase Proton Affinities (PA) and Gas Basicities (GB) in kcal mol$^{-1}$, Together with the p$K_a$ Values Calculated in MeCN Obtained at the M06-2X/6-311++G(2df,2pd)//M06-2X/6-31+G(d,p) Level of Theory[a]**

| | gas phase | | | acetonitrile | |
|---|---|---|---|---|---|
| system | $E_{EL}$ | PA | GB | $E_{EL}$ | p$K_a$ |
| **1A** | 0.0 | 258.2 | 249.5 | 0.0 | 23.9 |
| **1B** | not stable: goes to **1A** | | | 0.5 | |
| **1A-H$^+$** | 0.0 | 143.5 | 136.5 | 0.0 | 2.8 |
| **1B−H$^+$** | not stable: goes to **1A-H$^+$** | | | 2.6 | |
| **1C−H$^+$** | not stable: goes to **1A-H$^+$** | | | not stable: goes to **1A-H$^+$** | |
| **1D-H$^+$** | 26.9 | | | 21.3 | |
| **1A-$H_2^{2+}$** | 0.0 | | | 0.0 | |
| **1B−$H_2^{2+}$** | not stable: goes to **1A-$H_2^{2+}$** | | | 0.4 | |
| **2A** | 0.0 | 268.5 | 259.0 | 1.0 | |
| **2B** | 7.0 | | | 2.1 | |
| **2C** | 4.3 | | | 0.0 | 25.0 |
| **2A-H$^+$** | 0.0 | 195.5 | 188.6 | 0.0 | 20.5 |
| **2B-H$^+$** | not stable: goes to **2A-H$^+$** | | | not stable: goes to **2A-H$^+$** | |
| **3A-$H_2^{2+}$** | 0.0 | | | 0.7 | |
| **3B-$H_2^{2+}$** | 0.3 | | | 0.0 | |
| **3C-$H_2^{2+}$** | 1.4 | | | 1.3 | |
| $H_2C\{hpp\}_2$ (g) | | 267.2 | 259.6 | | 28.2 |
| $[H_2C\{hpp\}\{hppH\}]^+$ ([g-H]$^+$) | | 174.0 | 167.0 | | 15.2 |

[a] $E_{EL}$ denotes total electronic energy given in relative fashion (M06-2X/6-31+G(d,p) results, in kcal mol$^{-1}$).

The stabilities of the hypothetical pyridine-protonated species **1C-H$^+$** and **1D-H$^+$** are dependent on the orientation of the pyridyl group. Thus, **1C-H$^+$** is unstable in the gas phase, with the H$^+$ spontaneously transferred to the more basic imino nitrogen to generate **1A-H$^+$**. In contrast, **1D-H$^+$** (in which the pyridyl group is in an unfavorable conformation with respect to proton transfer) is stable albeit higher in energy than **1A-H$^+$** by 26.9 kcal mol$^{-1}$.

The calculated proton affinity of **1** in the gas phase, $PA_1$(**1**), is 258.2 kcal mol$^{-1}$. It is higher than those calculated for guanidine (PA = 235.8), pentamethylguanidine (PA = 250.7) and pyridine (PA = 220.8), which are found in excellent agreement with experimental values of 235.7, 250.4, and 222.0 kcal mol$^{-1}$, respectively.[62] Moreover, by comparing this value to that calculated for hppMe using the same model, 254.2 kcal mol$^{-1}$, we note that the pyridyl group increases the basicity by around 4.0 kcal mol$^{-1}$, which represents a significant increase. The IHB with the pyridyl moiety in **1A-H$^+$** manifests with a lengthening of the N1−H bond from 1.007 Å in [hppMe(H)]$^+$ to 1.027 Å.

A second protonation of **1** is possible to afford the dication, calculated as **1A-$H_2^{2+}$** and **1B-$H_2^{2+}$**. Interestingly, the rotamer in which the two positively charged NH groups are most distant (**1B-$H_2^{2+}$**) is unstable and spontaneously converts to the **1A-$H_2^{2+}$** isomer. The twist is very pronounced, |Φ(1)| = 50.2°, with a correspondingly large N1·····N4 distance of 2.942 Å. As expected, the gas-phase basicity of the second protonation is low, calculated as $PA_2$(**1**) = 143.5 kcal mol$^{-1}$. The lack of an IHB causes the N1−H distance to relax back to 1.013 Å.

*Disubstituted Derivatives Based on Compound II (Gas Phase).* The most stable calculated geometry of **2** in the gas-phase has both imino nitrogen atoms pointed away from the pyridine nitrogen (**2A**, Figure 13); this agrees with X-ray diffraction data.[24] The first protonation occurs exclusively on one imino nitrogen (N1), which optimizes as **2A-H$^+$** with formation of two IHBs to the pyridyl nitrogen N7 and the remaining imino group, N4. All parameters associated with the imino groups correlate reasonably well with the solid-state derived models (Table 3), italicized here in parentheses. The N1···N4 distance between imino nitrogen atoms is 3.042 Å (*3.129(1) Å*), with distances to the pyridyl nitrogen N7 of 2.714 Å (*2.692(1) Å*) and 2.783 Å (*2.811(1) Å*) for the protonated and neutral groups, respectively (Figure 14a). The angles at the hydrogen atom are 150.1° (*146.8(1)°*) and 124.4° (*132.1(2)°*) for the intramolecular hydrogen bond to the imino and pyridyl groups, respectively. Similar to the situation noted for **1C-H$^+$**/**1A-H$^+$**, protonation at the pyridyl nitrogen of **2B**



DOI: 10.1021/acs.joc.6b01330
J. Org. Chem. 2016, 81, 7612−7625

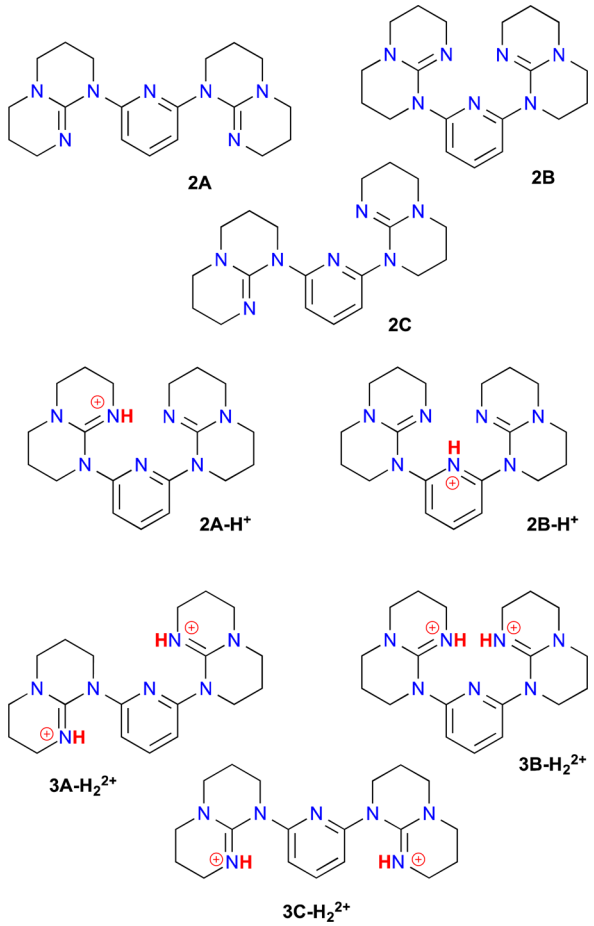


**Figure 13.** Conformers of **II**, [**II**-H]$^+$, and [**II**-H$_2$]$^{2+}$ used for computational analysis.

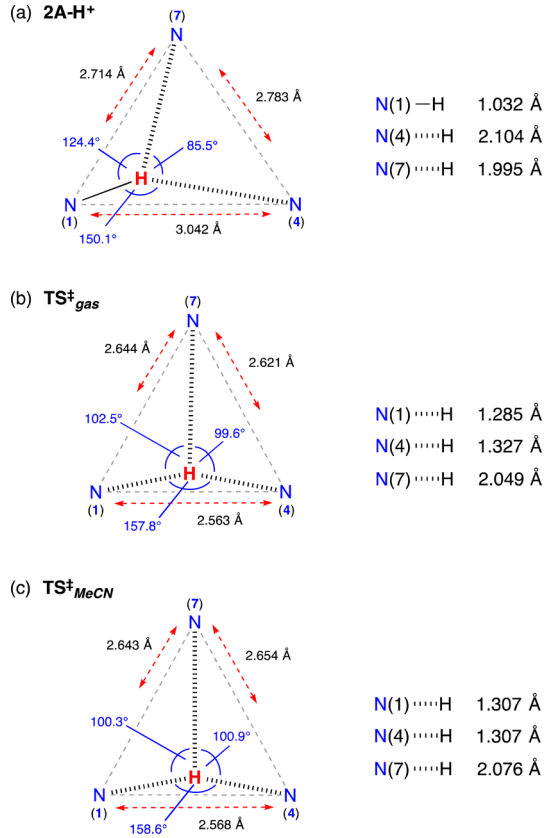


**Figure 14.** Scale diagrams of the core of (a) **2A**-H$^+$, (b) **TS**$^‡_{gas}$ and (c) **TS**$^‡_{MeCN}$ in implicit acetonitrile solution with 15 explicit MeCN molecules.

generates an unstable structure (**2B**-H$^+$), which undergoes spontaneous proton transfer to form **2A**-H$^+$.

The calculated gas-phase proton affinity for **2**, PA$_1$(**2**), is 268.5 kcal mol$^{-1}$. This is higher than calculated for **1**, and this increase is attributed to the presence of the second imino group and formation of two IHBs. It is encouraging to note that this value is greater than calculated for H$_2$C{hpp}$_2$ (**g**), which at the same level of theory gave PA$_1$(**g**) = 267.2 kcal mol$^{-1}$. This is despite a more favorable alignment for the formation of a strong IHB calculated in **g** (N1···N4 2.683 Å, N1—H···N4 176.2°) and is attributed to the pyridyl group playing an active role in stabilizing the conjugate acid, [**2**-H]$^+$. At 1.3 kcal mol$^{-1}$, the magnitude of this difference is within the error estimated by Kolboe for the M06-2X DFT functional, which is approximately 0.5 kcal mol$^{-1}$ for calculating proton affinities.[63]

The free energy barrier to the transfer of the proton to the neutral imino group in **2A**-H$^+$ (i.e., N1—H···N4 ↔ N1···H—N4) is $\Delta G^‡$ = +5.7 kcal mol$^{-1}$ ($\nu_{IMAG}$ = −1111 *i*cm$^{-1}$), which is

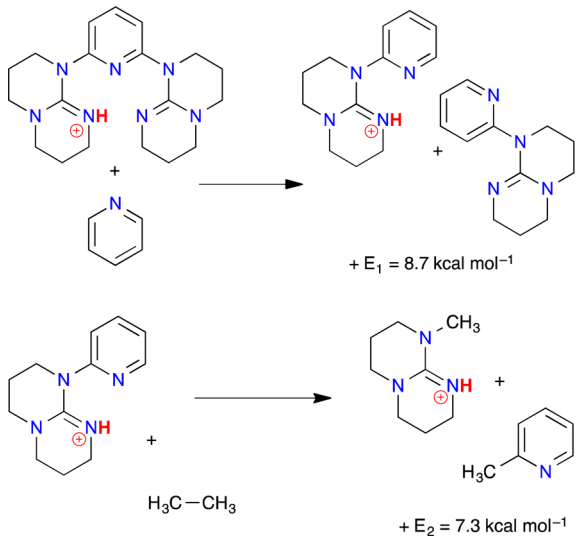


**(1)**

**(2)**



DOI: 10.1021/acs.joc.6b01330
J. Org. Chem. 2016, 81, 7612−7625

considerably higher than that calculated for [**g**-H]$^+$ (+2.5 kcal mol$^{-1}$).[22] This value is too large for spontaneous proton shuttle between the imino groups, meaning that at room temperature less than 0.01% of molecules exist with the proton at the N4 position. The calculated gas-phase transition state ($TS^{\ddagger}_{gas}$) for this process involves both $N_{imino}$ atoms with no participation from the pyridyl nitrogen atom. The N1····N4 distance (2.563 Å) is reduced significantly compared with the distance in **2A-H**$^+$ (N1····N4 = 3.042 Å). The N−H distances in $TS^{\ddagger}_{gas}$, however, are not symmetrical with N1···H and N4···H at 1.285 and 1.327 Å, respectively (Figure 14b). The distance between the transferring proton and the pyridyl nitrogen N7 is larger in $TS^{\ddagger}_{gas}$ (2.049 Å) than the optimized structure of **2A-H**$^+$ (1.995 Å). This confirms that the pyridyl group does not participate in proton transfer in the gas phase, resulting in a higher barrier than in [**g**-H]$^+$, but is involved in stabilization of [**II**-H]$^+$, making it more basic than [**g**-H]$^+$.

A useful method that we have used to estimate the interaction between molecular fragments derives from the concept of homodesmotic reactions,[64] which for **2A-H**$^+$ is summarized in eqs 1 and 2. The results indicate that the second hpp group and the pyridine fragment contribute almost equally to the proton affinity of **2**, with calculated values of 8.7 and 7.3 kcal mol$^{-1}$, respectively. This is a good qualitative agreement with the difference in the PA values for **2** and hppMe, being 14.3 kcal mol$^{-1}$.

The second protonation of **2** to afford **3** was also examined computationally. The most stable structure was found to be that in which one of the protonated imine groups points toward the pyridyl nitrogen and the other is rotated away (**3A-H$_2$**$^{2+}$). This does not agree with the structure observed in the solid-state X-ray-derived model, **3B-H$_2$**$^{2+}$, although this is only 0.3 kcal mol$^{-1}$ more stable in the gas phase. While it is questionable whether this difference is meaningful at this level of calculation, it prompted us to perform additional experiments with [$BPh_4$]$^-$ anions included (taking initial coordinates from the X-ray diffraction data). The results from these calculations indicate that conformation **3B-H$_2$**$^{2+}$ is more stable than **3A-H$_2$**$^{2+}$ by 1.8 kcal mol$^{-1}$, having two nonsymmetrical N1···N7 and N4···N7 distances of 2.659 and 2.746 Å, respectively. This once again agrees well with the model refined against X-ray diffraction data and underlines the important role of the [$BPh_4$]$^-$ counterions in the crystal packing.

*Conformations and Basicity Constants in Acetonitrile Solution.* Acetonitrile is a solvent of sufficient polarity to stabilize several conformations that are otherwise not observable in the gas-phase calculations (Table 5). This holds for **1B**, **1B-H**$^+$, and **1B-H$_2$**$^{2+}$, with the order of stabilities among conformations preserved in both gas and solution phases. An important exception to this is **3B-H$_2$**$^{2+}$, which was shown to be less stable than **3A-H$_2$**$^{2+}$ in the gas phase but is more stable when calculated in acetonitrile. This is in line with experimental solid-state data.

The calculated p$K_a$ value for the first protonation of **1** in MeCN, p$K_{a1}$(**1**) = 23.9 (Table 5). A second protonation of **1** that must occur at the pyridine nitrogen has also been calculated, and as expected, this value is much lower, p$K_{a2}$(**1**) = 2.8. This explains why the second protonation of **1** is not observed in solution using [$HNEt_3$][$BPh_4$], as the experimentally determined p$K_a$ value of [$HNEt_3$]$^+$ in acetonitrile is 10.72.[65]

The corresponding p$K_{a1}$(**2**) value is 25.0, commensurate with the presence of the second hpp unit. Curiously, the second value, p$K_{a2}$(**2**) = 20.5, is only slightly lower. We note that the autoprotolysis constant of acetonitrile at room temperature is very low: p$K_a$(auto) ≥ 33.[66] When these data are considered together with the p$K_a$ of [$HNEt_3$]$^+$, the calculated p$K_a$ values offer convincing evidence that both the mono- and diprotonated species **2-H**$^+$ and **3-H$_2$**$^{2+}$ are stable in acetonitrile solution and that they can be generated with 1 or 2 equiv of acidic [$HNEt_3$]$^+$ salts, respectively, as demonstrated in this study.

In implicit MeCN solution, the calculated position of the hydrogen atom for the transition state associated with **2A-H**$^+$ is more symmetrical than in the gas-phase calculations, with N1··· H and N4···H distances of 1.313 and 1.333 Å. The distance to the pyridyl nitrogen remains high (2.132 Å), which appears to contradict our conclusions from solution state $^{15}$N NMR data (vide supra), in which a shift of the resonance for the pyridyl nitrogen was interpreted as a contribution from this group to the proton transfer (**ii**, Scheme 3). This prompted us to include explicit acetonitrile molecules embedded in implicit solvation. After performing molecular dynamics simulations with **2A-H**$^+$ placed in a box of 483 explicit MeCN molecules, we selected a snapshot with the lowest energy and extracted a system containing 15 solvent molecules closest to the N1 protonation center. DFT analysis on this cluster (Figure 15) gave a

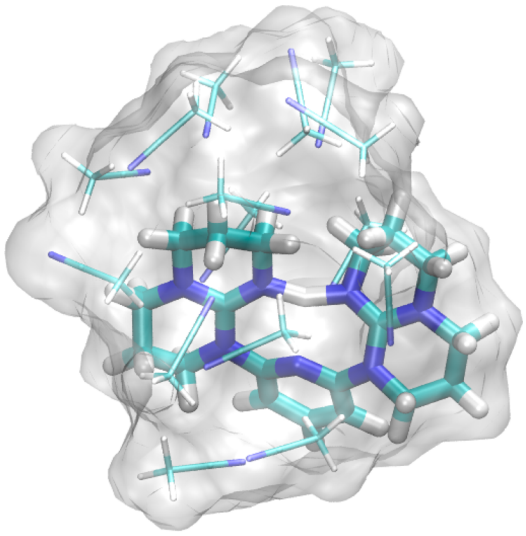

**Figure 15.** Optimized structure of the transition state for the proton transfer between N1 and N4 imino centers in the **2A-H**$^+$ system in a cluster of 15 acetonitrile molecules obtained at the (SMD)/M06-2X/6-31+G(d) level of theory.

symmetrical transition state with both N1···H and N4···H distances of 1.307 Å, while the distance to the pyridyl nitrogen dropped to 2.076 Å (Figure 14c), placing our results in closer agreement with earlier conclusions.

The barrier to proton transfer calculated in implicit MeCN is higher than in the gas -phase ($\Delta G^{\ddagger}$ = +9.1 kcal mol$^{-1}$). This appears to contradict the NMR data from which we are unable to distinguish between the two hpp groups in solution. However, the calculations with 15 explicit MeCN molecules brought the barrier down to +4.6 kcal mol$^{-1}$ ($\nu_{IMAG}$ = −1410 *i*cm$^{-1}$), an order of magnitude lower than in the gas phase ($\Delta G^{\ddagger}$ = +5.7 kcal mol$^{-1}$). Since analogous calculations with only one and two explicit MeCN molecules gave barriers of +8.8 and +5.5 kcal mol$^{-1}$, respectively, these results underline



DOI: 10.1021/acs.joc.6b01330
J. Org. Chem. 2016, 81, 7612−7625

the importance of including explicit solvation in accurately studying proton transfer phenomena. They also indicate a trend in calculated free energy barriers that rationalizes the observation that experimental results in solution are consistent with a facile proton transfer between imino nitrogen atoms in **2A-H**$^+$.

**Spectrophotometric Analysis of I and II.** The acidic dissociation of [**I**-H]$^+$ and [**II**-H]$^+$ in acetonitrile has been measured using UV−vis spectrophotometric titrations to authenticate the calculations presented above. As compound **I** could not be obtained in a pure form and was oily in nature, the measurements were performed with an isolated sample of [**I**-H]$^+$. To avoid complications in the spectra due to the presence of phenyl groups in $[BPh_4]^-$, the cation was provided as the $[PF_6]^-$ salt, **1b**. The experimental procedures are well established,[67−69] and a summary of the results is presented in Table 6.

**Table 6. Measured Acetonitrile p$K_a$ Values for [I-H]$^+$ and [II-H]$^+$ with Reference to Standards Shown in Figure 16**

| base (B) | reference base (Rb) | p$K_a$ (Rb) | $\Delta pK_a$[a] | p$K_a$(B) | assigned p$K_a$(B) |
|---|---|---|---|---|---|
| **I** | 2-Cl-$C_6H_4$-$P_2$(pyrr) | 25.42 | 1.12 | 24.30 | 24.1 |
| | 4-$CF_3$-$C_6H_4$-$P_2$(pyrr) | 25.29 | 1.16 | 24.13 | |
| | 2-Cl-$C_6H_4$-$P_2$(dma) | 24.23 | 0.15 | 24.08 | |
| **II** | 2-Cl-$C_6H_4$-$P_2$(pyrr) | 25.42 | −0.18 | 25.60 | 25.6 |
| | 4-$CF_3$-$C_6H_4$-$P_2$(pyrr) | 25.29 | −0.31 | 25.60 | |
| | 2-Cl-$C_6H_4$-$P_2$(dma) | 24.23 | 0.56 | 25.90 | |

[a] p$K_a$(Rb) − p$K_a$(B).

Measurements for [**I**-H]$^+$ and [**II**-H]$^+$ were made against three phosphazene reference compounds of known p$K_a$ (Figure 16).[3] The experimentally determined results are in excellent

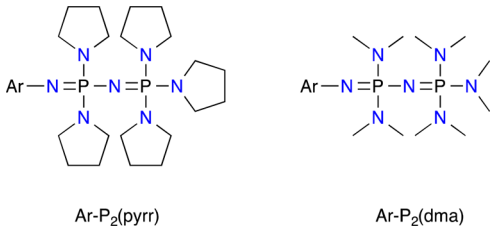


**Figure 16.** Reference bases used to determine the p$K_a$ values of **I** and **II** in acetonitrile solution (Ar = 2-Cl-$C_6H_4$ and 4-$CF_3$-$C_6H_4$).

agreement with the calculated values for **I** (p$K_a$(obs) = 24.1; p$K_a$(calcd) = 23.9) and **II** (p$K_a$(obs) = 25.6; p$K_a$(calcd) = 25.0), validating the computational models. As expected, the presence of a second hpp group increases the basicity, although the value of **II** is still considerably lower than our previously studied system, $H_2C\{hpp\}_2$ (p$K_a$(obs) = 29.0). We also acknowledge the role that size plays in determining the basicity of a system.[70] Thus, a contributing factor why **II** is more basic than **I** in the gas phase, while less basic in MeCN, derives from the fact that larger systems and larger electron-donating substituents lead to an increase in the intrinsic electronic effect (relevant for increasing the gas-phase basicity) but also decrease the solvent stabilization (relevant for diminishing basicity in solution).

## CONCLUSIONS

We have successfully demonstrated that using pyridine to support one or two hpp units affords new organic superbases. $^{15}N$ NMR spectroscopy was identified as a useful technique in the characterization of the guanidinium salts, with a large upfield shift evident for the protonated imino nitrogen atom. A more subtle shift in the transannular nitrogen resonance (N3/N6) was interpreted as indicating a large contribution from the $\gamma$-resonance. This postulate was supported by computational data, where the NBO atomic charges in **1A-H**$^+$ on N1 (−0.68 |el|), N2 (−0.53 |el|) and N3 (−0.54 |el|) atoms change to N1 (−0.67 |el|), N2 (−0.49 |el|) and N3 (−0.47 |el|) upon protonation, confirming the greatest increase in charge occurs at N3. The charge on the pyridyl nitrogen undergoes only a modest change from −0.52 to −0.54 |el|. Likewise in **2A-H**$^+$ the N3 atom of the protonated guanidinium groups accommodates most of the excess positive charge in the [hpp-H]$^+$ unit. Its NBO charge changes from −0.53 to −0.47 |el| upon protonation, while all other nitrogen atoms increase their charge by only up to +0.03 |el|.

Changes in the bond C−N bond lengths from X-ray diffraction data are consistent with related protonation experiments. However, the acquisition of neutron diffraction data enabled the role of inter- and intramolecular H···H interactions to be accurately assessed for the first time. This allowed the observed torsion angles between the hpp- and the pyridyl-components to be explained as arising from a hitherto unrecognized and remote steric clash between C−H···H−C atoms that are likely to influence the overall basicity.

In the gas phase, the proton affinity of **II** is the highest recorded for a compound containing the hpp unit, exceeding the values previously reported for the methylene-linked example, $H_2C\{hpp\}_2$ (**g**). However, a lower p$K_a$ value was measured in acetonitrile relative to **g**. Computational analysis was used to rationalize these observations. While the pyridine group forms stabilizing interactions with the protonation center, thereby increasing the gas-phase basicity (vide supra), in solution these interactions are significantly reduced. Furthermore, the bulk inherent in the [**I**-H]$^+$ molecule prevents MeCN molecules from efficiently stabilizing the positive charge in solution, both resulting in diminished p$K_a$ values. These results underline the crucial role of explicit solvation for an accurate treatment of the system.

## EXPERIMENTAL SECTION

**General Information.** All manipulations were carried out under dry nitrogen using standard Schlenk line and cannula techniques or in a conventional nitrogen-filled glovebox. Solvents were dried over appropriate drying agents and degassed prior to use. NMR spectra were recorded at 300.1, 500.1, or 600.1 MHz ($^1H$), 75.4, 125.4, or 150.9 MHz ($^{13}C$), 282.2 MHz ($^{19}F$), 121.4 MHz ($^{31}P$), and 60.8 MHz ($^{15}N$). $^{15}N$ NMR spectra were recorded using a triple-resonance HCN cryogenic probe operating at 25 K. Proton and carbon chemical shifts were referenced internally to residual solvent resonances and all coupling are reported in Hz. $^{15}N$ chemical shifts in solution were assigned using a combination of $^1H-^{13}C$ TOCSY, 2D NOESY and $^1H-^{15}N$ CIGAR experiments. Melting points were measured in sealed glass capillaries under a $N_2$ atmosphere and are uncorrected. IR spectra were recorded as Nujol mulls between KBr plates. Compounds **I**,[30] **II**,[25] and $[HNEt_3][BPh_4]$[33] were synthesized according to literature procedures. Compound **I** was isolated as a colorless oil of ∼90% purity and was used without further purification.

*Data for 2-{hpp}$C_5H_4N$ (I).* $^1H$ NMR ($CD_3CN$, 300 MHz): $\delta$ 8.18 (ddd, 1H, $J$ = 4.9, 1.9 and 0.77, $C_5H_4N$), 7.59 (d, 1H, $J$ = 8.5, $C_5H_4N$),



DOI: 10.1021/acs.joc.6b01330
J. Org. Chem. 2016, 81, 7612−7625

7.46 (ddd, 1H, $J$ = 8.6, 7.1 and 2.0, $C_5H_4N$), 6.80 (ddd, 1H, $J$ = 7.0, 4.9 and 0.98, $C_5H_4N$), 3.76, 3.26, 3.20, 3.15, 1.97, 1.81 (m, 2H, hpp-$CH_2$). $^{13}C\{^1H\}$ NMR ($CD_3CN$, 75 MHz): $\delta$ 157.9 ($CN_3$), 149.3, 147.6, 135.9, 120.9, 117.3 ($C_5H_4N$), 49.4, 49.0, 44.4, 44.3, 24.3, 23.4 (hpp-$CH_2$). $^{15}N$ NMR ($CD_3CN$, 60.8 MHz): $\delta$ −96.2 (*N*4), −207.3 (*N*1), −278.4 (*N*2), −308.1 (*N*3). IR 1625 (m), 1600 (s), 1587 (s), 1562 (m) (C═N) $cm^{-1}$.

*Data for 2,6-{hpp}$_2C_5H_3N$ (**II**).* $^1H$ NMR ($CD_3CN$, 300 MHz): $\delta$ 7.28 (dd, 1H, $J$ = 7.5, *p*-$C_5H_3N$), 7.07 (m, 2H, *m*-$C_5H_3N$), 3.74, 3.25, 3.18, 3.13, 1.95, 1.79 (m, 4H, hpp-$CH_2$). $^{13}C\{^1H\}$ NMR ($CD_3CN$, 75 MHz): $\delta$ 155.5 ($CN_3$), 150.2, 136.1, 111.7 ($C_5H_3N$), 49.2, 48.9, 44.3, 44.2, 24.1, 23.3 (hpp-$CH_2$). $^{15}N$ NMR ($CD_3CN$, 60.8 MHz): $\delta$ −116.8 (*N*7), −206.1 (*N*1/*N*4), −279.8 (*N*2/*N*5), −308.4 (*N*3/*N*6). IR 1621 (s), 1572 (s) (C═N) $cm^{-1}$.

*Preparation of [2-{hppH}$C_5H_4N$][$BPh_4$] ([I-H][$BPh_4$], **1a**).* A solution of [$HNEt_3$][$BPh_4$] (0.20 g, 0.47 mmol) in MeCN (5 mL) was added dropwise to a stirring solution of 2-{hpp}$C_5H_4N$ (**I**) (0.10 g, 0.46 mmol) in MeCN (5 mL) at room temperature. The mixture was stirred for 2 h, and the volatiles were removed under vacuum. The resulting oil was redissolved in MeCN, and the solvent was allowed to evaporate at ambient temperature to give colorless crystals of **1a**. Yield: 0.22 g, 89%. Mp: 156−157 °C. $^1H$ NMR ($CD_3CN$, 300 MHz): $\delta$ 9.47 (br, 1H, N*H*), 8.37 (dd, 1H, $J$ = 4.9 and 1.2, $C_5H_4N$), 7.87 (td, 1H, $J$ = 8.36 and 2.0, $C_5H_4N$), 7.27 (br m, 10H, *o*-$C_6H_5$ and $C_5H_4N$), 7.21 (d, 1H, $J$ = 8.4, $C_5H_4N$), 6.99 (t, 8H, $J$ = 7.4, *m*-$C_6H_5$) 6.84 (t, 4H, $J$ = 7.4, *p*-$C_6H_5$), 3.65 (m, 2H, hpp-$CH_2$), 3.29 (m, 6H, hpp-$CH_2$), 2.05, 1.89 (m, 2H, hpp-$CH_2$). $^{13}C\{^1H\}$ NMR ($CD_3CN$, 75 MHz): $\delta$ 164.7 (4-line multiplet, $J_{CB}$ = 49.3, *i*-$C_6H_5$), 155.4 ($CN_3$), 148.2, 141.1 ($C_5H_4N$), 136.6 (*m*-$C_6H_5$), 127.4 ($C_5H_4N$), 126.5 (4-line multiplet, $J_{CB}$ = 2.7, *o*-$C_6H_5$), 122.7 (*p*-$C_6H_5$), 122.5, 117.3 ($C_5H_4N$), 48.9, 48.3, 47.5, 39.4, 21.4, 20.5 (hpp-$CH_2$). $^{15}N$ NMR ($CD_3CN$, 60.8 MHz): $\delta$ −96.7 (*N*4), −281.9 (*N*2), −295.3 (*N*3), −298.5 (*N*1-H). IR: 3222 (w, N−H), 1618 (s), 1601 (s), 1584 (s), 1569 (s) (C═N) $cm^{-1}$. Anal. Calcd for $C_{36}H_{37}BN_4$ (536.53): C, 80.59; H, 6.95; N, 10.44. Found: C, 80.50; H, 7.04; N, 10.34.

*Preparation of [2-{hppH}$C_5H_4N$][$PF_6$] ([I−H][$PF_6$], **1b**).* Compound **1b** was prepared according to the procedure outlined for **1a** using $NH_4PF_6$ (0.33 g, 2.04 mmol) and 2-{hpp}$C_5H_4N$ (I) (0.44 g, 2.04 mmol). A white precipitate formed during the addition, and the resulting suspension was stirred for 2 h. Removal of the volatiles under vacuum afforded a colorless oil that was extracted into THF (7 mL), warmed to 40 °C in a water bath, and allowed to cool slowly to room temperature to give colorless crystals of **1b**. Yield: 0.56 g, 76%. Mp: 166−169 °C. $^1H$ NMR ($CD_3CN$, 300 MHz): $\delta$ 9.43 (br, 1H, N*H*), 8.44 (dd, 1H, $J$ = 4.6 and 1.3, $C_5H_4N$), 7.95 (t, 1H, $J$ = 7.1, $C_5H_4N$), 7.32 (m, 2H, $C_5H_4N$), 3.79 (m, 2H, hpp-$CH_2$), 3.43 (m, 4H, hpp-$CH_2$), 3.35, 2.17, 1.99 (m, 2H, hpp-$CH_2$). $^{13}C\{^1H\}$ NMR ($CD_3CN$, 75 MHz): $\delta$ 155.4 ($CN_3$), 151.7, 148.3, 141.0, 122.5, 117.5 ($C_5H_4N$), 48.9, 48.3, 47.6, 39.4, 21.5, 20.5 (hpp-$CH_2$). $^{31}P$ NMR ($CD_3CN$, 121 MHz): $\delta$ −139.4 (sept, $J$ = 706.8). $^{19}F$ NMR ($CD_3CN$, 282.2 MHz): $\delta$ −72.9 (d, $J$ = 706.8). Anal. Calcd for $C_{12}H_{17}F_6N_4P$ (362.26): C, 39.79; H, 4.73; N, 15.47. Found: C, 39.70; H, 4.65; N, 15.40.

*Preparation of [2-{hppH}-6-{hpp}$C_5H_3N$][$BPh_4$] ([II-H][$BPh_4$], **2**).* A solution of [$HNEt_3$][$BPh_4$] (0.12 g, 0.28 mmol) in MeCN (5 mL) was added dropwise to a stirring solution of 2,6-{hpp}$_2C_5H_3N$ (II) (0.10 g, 0.28 mmol) in MeCN (5 mL) at room temperature. The mixture was stirred for 1 h, and the volatiles were removed under vacuum. The resulting oil was extracted into THF, and the solvent was allowed to evaporate at ambient temperature to give colorless crystals of **2**. Yield: 0.16 g, 84%. Mp: 173−175 °C. $^1H$ NMR ($CD_3CN$, 300 MHz): $\delta$ 7.86 (t, 1H, $J$ = 7.2, *p*-$C_5H_3N$), 7.28 (br m, 8H, *o*-$C_6H_5$), 7.10 (d, 2H, $J$ = 7.2, *m*-$C_5H_3N$), 7.00 (t, 8H, $J$ = 7.2, *m*-$C_6H_5$), 6.85 (t, $J$ = 7.2, 4H, *p*-$C_6H_5$), 3.66 (m, 4H, hpp-$CH_2$), 3.30 (m, 12H, hpp-$CH_2$), 2.06, 1.89 (m, 4H, hpp-$CH_2$). $^1H$ NMR ($CD_2Cl_2$, 300 MHz): $\delta$ 9.70 (br, 1H, N*H*), 7.70 (t, 1H, $J$ = 8.1, *p*-$C_5H_3N$), 7.33 (br, 8H, *o*-$C_6H_5$), 7.03 (t, 8H, $J$ = 7.3, *m*-$C_6H_5$), 6.88 (t, $J$ = 7.2, 4H, *p*-$C_6H_5$), 6.77 (t, $J$ = 8.1, 2H, *m*-$C_5H_3N$), 3.56, 3.31, 3.20, 3.13, 2.00, 1.85 (m, 4H, hpp-$CH_2$). $^{13}C\{^1H\}$ NMR ($CD_3CN$, 75 MHz): $\delta$ 164.7 (4-line multiplet, $J_{CB}$ = 49.3, *i*-$C_6H_5$), 154.3 ($CN_3$), 150.8, 141.3, 136.7 (4-line multiplet, $J_{CB}$ = 1.4, $C_6H_5$), 126.5 (4-line multiplet, $J_{CB}$ = 2.8, $C_6H_5$), 122.7, 112.4 ($C_5H_3N$), 48.9, 48.7, 46.7, 42.4, 22.8, 21.9 (hpp-$CH_2$). $^{15}N$ NMR ($CD_3CN$, 60.8 MHz): $\delta$ −109.6 (*N*7), −280.7 (*N*1-H/*N*4), −282.0 (*N*2/*N*5), −297.4 (*N*3/*N*6). IR: 3240 (N−H), 1630 (s), 1594 (s), 1568 (m) (C═N) $cm^{-1}$. Anal. Calcd for $C_{43}H_{48}BN_7$ (673.72): C, 76.66; H, 7.18; N, 14.55. Found: C, 76.53; H, 7.22; N, 14.45.

*Preparation of [2,6-{hppH}$_2C_5H_3N$][$BPh_4$]$_2$ ([II-$H_2$][$BPh_4$]$_2$, **3**).* Compound **3** was prepared according to the procedure outlined for **2** using [$HNEt_3$][$BPh_4$] (0.24 g, 0.56 mmol) and 2,6-{hpp}$_2C_5H_3N$ (II) (0.10 g, 0.28 mmol). The mixture was stirred for 1 h, and the volatiles were removed under vacuum. The resulting oil was extracted into MeCN, and the solvent was allowed to evaporate at ambient temperature to give crystals of **3**. Yield: 0.42 g, 78%. Mp: 216−218 °C. $^1H$ NMR ($CD_3CN$, 300 MHz): $\delta$ 7.97 (t, $J$ = 8.1, 1H, *p*-$C_5H_3N$), 7.29 (br, 16H, *o*-$C_6H_5$), 7.19 (d, $J$ = 8.1, 2H, *m*-$C_5H_3N$), 7.01 (t, 16H, $J$ = 7.5, *m*-$C_6H_5$), 6.86 (t, $J$ = 7.2, 8H, *p*-$C_6H_5$), 3.63 (m, 4H, hpp-$CH_2$), 3.34 (m, 8H, hpp−$CH_2$), 3.22, 2.07, 1.91 (m, 4H, hpp-$CH_2$). $^{13}C$ NMR ($CD_3CN$, 75 MHz): $\delta$ 164.7 (4-line multiplet, $J_{CB}$ = 49.4, *i*-$C_6H_5$), 153.0 ($CN_3$), 151.4, 144.3, 136.6 (4-line multiplet, $J_{CB}$ = 1.3, $C_6H_5$)), 126.5 (q, $J_{CB}$ = 2.76, $C_6H_5$), 122.7, 118.0 ($C_5H_3N$), 48.7, 48.4, 48.0, 39.5, 21.6, 20.5 (hpp-$CH_2$). $^{15}N$ NMR ($CD_3CN$, 60.8 MHz): $\delta$ −106.9 (*N*7), −282.5 (*N*2/*N*5), −293.4 (*N*3/*N*6), −300.1 (*N*1-H/*N*4-H). IR: 3379 (N−H), 1624 (s), 1590 (s), 1559 (m) (C═N) $cm^{-1}$. Anal. Calcd for $C_{67}H_{69}B_2N_7$ (993.96): C, 80.96; H, 7.00; N, 9.86. Found: C, 81.15; H, 6.87; N, 9.95.

## ■ ASSOCIATED CONTENT

### Ⓢ Supporting Information

The Supporting Information is available free of charge on the ACS Publications Web site at DOI: XXXXXX. $^1H$, $^{13}C$, and $^{15}N$ NMR spectra; computational details and atomic coordinates; a crystallographic information file (cif) containing X-ray diffraction data for **1a**, **1b**, **2**, **3** and neutron diffraction data for **1a** The Supporting Information is available free of charge on the ACS Publications website at DOI: 10.1021/acs.joc.6b01330.

$^1H$, $^{13}C$, and $^{15}N$ NMR spectra; computational details and atomic coordinates; neutron diffraction data for **1a** (PDF)

X-ray diffraction data for **1a**,**b**, **2**, and **3** (CIF)

## ■ AUTHOR INFORMATION


### Corresponding Authors

*E-mail: robert.vianello@irb.hr.

*E-mail: martyn.coles@vuw.ac.nz.


### Notes

The authors declare no competing financial interest.

## ■ ACKNOWLEDGMENTS

We acknowledge the assistance of Dr. Peter Northcote and Ian Vorster during the acquisition of solution-state $^{15}N$ NMR spectra. R.J.S. acknowledges the award of a Victoria University of Wellington Ph.D. Scholarship and a Curtis−Gordon Scholarship. We thank AINSE Ltd. for providing financial assistance (Award PGRA) to enable work on single-crystal neutron diffraction. M.P.C. acknowledges financial support from a VUW University Research Fund grant. The Australian Nuclear Science and Technology Organization is thanked for the award of neutron beam time on KOALA to proposal P3391. R.V. acknowledges the European Commission for a Marie Curie FP7 Career Integration Grant (Contract No. PCIG12-GA-2012-334493). A.M. thanks the Croatian Science Foundation for a doctoral stipend through the Career Development Project for Young Researchers (Contract No. I-3376-2014). M.A.G. and R.M.C. are grateful to the Ministerio



DOI: 10.1021/acs.joc.6b01330
J. Org. Chem. 2016, 81, 7612−7625

de Economía y Competitividad of Spain (Project No. CTQ2014-56833R) for financial support. The work of I.L. and J.S. was supported by the institutional research funding IUT14-20 (TLOKT14014I) from the Estonian Ministry of Education and Research.

## REFERENCES


(1) Margetic, D. In *Superbases for Organic Synthesis: Guanidines, Amidines, Phosphazenes and Related Organocatalysts*; Ishikawa, T., Ed.; Wiley: Chichester, 2009; pp 9−48.
(2) All p$K_a$ values in this manuscript are experimentally determined in MeCN solution unless otherwise stated.
(3) Kaljurand, I.; Kütt, A.; Sooväli, L.; Rodima, T.; Mäemets, V.; Leito, I.; Koppel, I. A. *J. Org. Chem.* **2005**, *70*, 1019−1028.
(4) Alder, R. W.; Bowman, P. S.; Steele, W. R. S.; Winterman, D. R. *Chem. Commun. (London)* **1968**, 723−724.
(5) Schwesinger, R. *Nachr. Chem., Tech. Lab.* **1990**, *38*, 1214−1226.
(6) Raab, V.; Kipke, J.; Gschwind, R. M.; Sundermeyer, J. *Chem. - Eur. J.* **2002**, *8*, 1682−1693.
(7) Barić, D.; Dragičević, I.; Kovačević, B. *J. Org. Chem.* **2013**, *78*, 4075−4082.
(8) Kovačević, B.; Glasovac, Z.; Maksić, Z. B. *J. Phys. Org. Chem.* **2002**, *15*, 765−774.
(9) Glasovac, Z.; Kovačević, B.; Meštrović, E.; Eckert-Maksić, M. *Tetrahedron Lett.* **2005**, *46*, 8733−8736.
(10) Eckert-Maksić, M.; Glasovac, Z.; Trošelj, P.; Kütt, A.; Rodima, T.; Koppel, I.; Koppel, I. A. *Eur. J. Org. Chem.* **2008**, *2008*, 5176−5184.
(11) Vazdar, K.; Kunetskiy, R.; Saame, J.; Kaupmees, K.; Leito, I.; Jahn, U. *Angew. Chem., Int. Ed.* **2014**, *53*, 1435−1438.
(12) The abbreviation hppH is derived from the IUPAC name, 1,3,4,6,7,8-hexahydro-2*H*-pyrimido[1,2-*a*]pyrimidine. This compound is also abbreviated as TBD, taken from the von Baeyer nomenclature, 1,5,7-triazabicyclo[4.4.0]dec-5-ene.
(13) Kiesewetter, M. K.; Scholten, M. D.; Kirn, N.; Weber, R. L.; Hedrick, J. L.; Waymouth, R. M. *J. Org. Chem.* **2009**, *74*, 9490−9496.
(14) Pratt, R. C.; Lohmeijer, B. G. G.; Long, D. A.; Waymouth, R. M.; Hedrick, J. L. *J. Am. Chem. Soc.* **2006**, *128*, 4556−4557.
(15) Coles, M. P. *Dalton Trans.* **2006**, 985−1001.
(16) Coles, M. P. *Chem. Commun.* **2009**, 3659−3676.
(17) Oakley, S. H.; Coles, M. P.; Hitchcock, P. B. *Inorg. Chem.* **2004**, *43*, 7564−7466.
(18) Sáez, P. J. A.; Oakley, S. H.; Coles, M. P.; Hitchcock, P. B. *Chem. Commun.* **2007**, 816−818.
(19) Khalaf, M. S.; Oakley, S. H.; Coles, M. P.; Hitchcock, P. B. *Dalton Trans.* **2010**, *39*, 1635−1642.
(20) Coles, M. P.; Hitchcock, P. B. *Chem. Commun.* **2007**, 5229−5231.
(21) Coles, M. P.; Lee, S. F.; Oakley, S. H.; Estiu, G.; Hitchcock, P. B. *Org. Biomol. Chem.* **2007**, *5*, 3909−3911.
(22) Coles, M. P.; Aragón-Sáez, P. J.; Oakley, S. H.; Hitchcock, P. B.; Davidson, M. G.; Maksić, Z. B.; Vianello, R.; Leito, I.; Kaljurand, I.; Apperley, D. C. *J. Am. Chem. Soc.* **2009**, *131*, 16858−16868.
(23) Pal, A. K.; Mandali, P. K.; Chand, D. K.; Hanan, G. S. *Synlett* **2015**, *26*, 1408−1412.
(24) Pal, A. K.; Serroni, S.; Zaccheroni, N.; Campagna, S.; Hanan, G. S. *Chem. Sci.* **2014**, *5*, 4800−4811.
(25) Pal, A. K.; Zaccheroni, N.; Campagna, S.; Hanan, G. S. *Chem. Commun.* **2014**, *50*, 6846−6849.
(26) Pal, A. K.; Ducharme, P. D.; Hanan, G. S. *Chem. Commun.* **2014**, *50*, 3303−3305.
(27) Pal, A. K.; Hanan, G. S. *Dalton Trans.* **2014**, *43*, 11811−11814.
(28) Pal, A. K.; Hanan, G. S. *Dalton Trans.* **2014**, *43*, 6567−6577.
(29) Pal, A. K.; Nag, S.; Ferreira, J. G.; Brochery, V.; La Ganga, G.; Santoro, A.; Serroni, S.; Campagna, S.; Hanan, G. S. *Inorg. Chem.* **2014**, *53*, 1679−1689.
(30) Nag, S.; Ferreira, J. G.; Chenneberg, L.; Ducharme, P. D.; Hanan, G. S.; La Ganga, G.; Serroni, S.; Campagna, S. *Inorg. Chem.* **2011**, *50*, 7−9.
(31) Glasovac, Z.; Pavošević, F.; Štrukil, V.; Eckert-Maksić, M.; Schlangen, M.; Kretschmer, R. *Int. J. Mass Spectrom.* **2013**, *354*−*355*, 113−122.
(32) Wolfe, J. P.; Buchwald, S. L. *J. Org. Chem.* **2000**, *65*, 1144−1157.
(33) Casely, I. J.; Ziller, J. W.; Mincher, B. J.; Evans, W. J. *Inorg. Chem.* **2011**, *50*, 1513−1520.
(34) Khalaf, M. S.; Oakley, S. H.; Coles, M. P.; Hitchcock, P. B. *CrystEngComm* **2008**, *10*, 1653−1661.
(35) Pawlak, Z.; Zundel, G.; Fritsch, J.; Wawrzynów, A.; Kuna, S.; Tusk, M. *Electrochim. Acta* **1984**, *29*, 391−395.
(36) Kolehmainen, E.; Ośmiałowski, B. *Int. Rev. Phys. Chem.* **2012**, *31*, 567−629.
(37) Städeli, W.; von Philipsborn, W. *Org. Magn. Reson.* **1981**, *15*, 106−109.
(38) Ghiviriga, I.; El-Gendy, B. E.-D. M.; Steel, P. J.; Katritzky, A. R. *Org. Biomol. Chem.* **2009**, *7*, 4110−4119.
(39) Coles, M. P.; Khalaf, M. S.; Claramunt, R. M.; García, M. A.; Alkorta, I.; Elguero, J. *J. Phys. Org. Chem.* **2010**, *23*, 526−535.
(40) Semenov, V. A.; Samultsev, D. O.; Krivdin, L. B. *Magn. Reson. Chem.* **2015**, *53*, 433−441.
(41) All $^{15}$N solution-state chemical shifts were assigned using a combination of $^{1}$H−$^{13}$C TOCSY, 2D-NOESY, and $^{1}$H−$^{15}$N CIGAR experiments.
(42) Kleinmaier, R.; Arenz, S.; Karim, A.; Carlsson, A.-C. C.; Erdélyi, M. *Magn. Reson. Chem.* **2013**, *51*, 46−53.
(43) Molecule **3a** contains the N7 pyridyl group, **3b** contains the N14 pyridyl group, and **3c** contains the N21 pyridyl group.
(44) Prelog, V.; Helmchen, G. *Angew. Chem., Int. Ed. Engl.* **1982**, *21*, 567−583.
(45) Coles, M. P.; Stokes, F. A.; Kingsbury, B. F. K.; Day, B. M.; Hitchcock, P. B. *Cryst. Growth Des.* **2011**, *11*, 3206−3212.
(46) Häfelinger, G.; Kuske, F. K. H., General and theoretical aspects of amidines and related compounds. In *Amidines and Imidates (1991)*; John Wiley & Sons, Ltd., 2010; pp 1−100.
(47) Coles, M. P.; Hitchcock, P. B. *Organometallics* **2003**, *22*, 5201−5211.
(48) Raab, V.; Harms, K.; Sundermeyer, J.; Kovačević, B.; Maksić, Z. B. *J. Org. Chem.* **2003**, *68*, 8790−8797.
(49) Kovačević, B.; Maksić, Z. B. *Chem. - Eur. J.* **2002**, *8*, 1694−1702.
(50) Allen, F. H.; Bruno, I. J. *Acta Crystallogr., Sect. B: Struct. Sci.* **2010**, *66*, 380−386.
(51) Edwards, A. J. *Aust. J. Chem.* **2011**, *64*, 869−872.
(52) Piltz, R. *Acta Crystallogr., Sect. A: Found. Crystallogr.* **2011**, *67*, C155.
(53) Wilson, C. C. *Single Crystal Neutron Diffraction from Molecular Materials*; World Scientific Publishing: Singapore, 1999.
(54) Betteridge, P. W.; Carruthers, J. R.; Cooper, R. I.; Prout, K.; Watkin, D. J. *J. Appl. Crystallogr.* **2003**, *36*, 1487.
(55) Bondi, A. *J. Phys. Chem.* **1964**, *68*, 441−451.
(56) Vazdar, M.; Vymětal, J.; Heyda, J.; Vondrášek, J.; Jungwirth, P. *J. Phys. Chem. A* **2011**, *115*, 11193−11201.
(57) Wallace, A. J.; Jayasinghe, C. D.; Polson, M. I. J.; Curnow, O. J.; Crittenden, D. L. *J. Am. Chem. Soc.* **2015**, *137*, 15528−15532.
(58) Despotovic, I.; Vianello, R. *Chem. Commun.* **2014**, *50*, 10941−10944.
(59) Zhao, Y.; Truhlar, D. G. *J. Chem. Theory Comput.* **2011**, *7*, 669−676.
(60) Picek, I.; Vianello, R.; Šket, P.; Plavec, J.; Foretić, B. *J. Org. Chem.* **2015**, *80*, 2165−2173.
(61) Saftić, D.; Vianello, R.; Žinić, B. *Eur. J. Org. Chem.* **2015**, *2015*, 7695−7704.
(62) Kaljurand, I.; Saame, J.; Rodima, T.; Koppel, I.; Koppel, I. A.; Kögel, J. F.; Sundermeyer, J.; Köhn, U.; Coles, M. P.; Leito, I. *J. Phys. Chem. A* **2016**, *120*, 2591−2604.
(63) Kolboe, S. *J. Chem. Theory Comput.* **2014**, *10*, 3123−3128.
(64) Wheeler, S. E. *Wiley Interdiscip. Rev. Comput. Mol. Sci.* **2012**, *2*, 204−220.
(65) Muckerman, J. T.; Skone, J. H.; Ning, M.; Wasada-Tsutsui, Y. *Biochim. Biophys. Acta, Bioenerg.* **2013**, *1827*, 882−891.




DOI: 10.1021/acs.joc.6b01330
*J. Org. Chem.* 2016, 81, 7612−7625

(66) Kolthoff, I. M.; Chantooni, M. K. *J. Phys. Chem.* **1968**, *72*, 2270−2272.
(67) Kaljurand, I.; Rodima, T.; Leito, I.; Koppel, I. A.; Schwesinger, R. *J. Org. Chem.* **2000**, *65*, 6202−6208.
(68) Leito, I.; Kaljurand, I.; Koppel, I. A.; Yagupolskii, L. M.; Vlasov, V. M. *J. Org. Chem.* **1998**, *63*, 7868−7874.
(69) Rodima, T.; Kaljurand, I.; Pihl, A.; Mäemets, V.; Leito, I.; Koppel, I. A. *J. Org. Chem.* **2002**, *67*, 1873−1881.
(70) Eberle, B.; Hübner, O.; Ziesak, A.; Kaifer, E.; Himmel, H.-J. *Chem. - Eur. J.* **2015**, *21*, 8578−8590.



DOI: 10.1021/acs.joc.6b01330
*J. Org. Chem.* 2016, 81, 7612−7625